

2017

Microscopic Evaluations of Bone in Equine and Muroid Models

Heather Ashley Richbourg

Louisiana State University and Agricultural and Mechanical College

Follow this and additional works at: https://digitalcommons.lsu.edu/gradschool_dissertations



Part of the [Medicine and Health Sciences Commons](#)

Recommended Citation

Richbourg, Heather Ashley, "Microscopic Evaluations of Bone in Equine and Muroid Models" (2017). *LSU Doctoral Dissertations*. 4395.

https://digitalcommons.lsu.edu/gradschool_dissertations/4395

This Dissertation is brought to you for free and open access by the Graduate School at LSU Digital Commons. It has been accepted for inclusion in LSU Doctoral Dissertations by an authorized graduate school editor of LSU Digital Commons. For more information, please contact gradetd@lsu.edu.

MICROSCOPIC EVALUATIONS OF BONE IN EQUINE AND MUROID MODELS

A Dissertation

Submitted to the Graduate Faculty of the
Louisiana State University and
Agricultural and Mechanical College
In partial fulfillment of the
requirements for the degree of
Doctor of Philosophy

in

Biomedical and Veterinary Medical Sciences through the
Department of Comparative Biomedical Sciences

by
Heather Ashley Richbourg
B.S., Young Harris College, 2013
May 2017

ACKNOWLEDGEMENTS

I would first like to thank my fiancé, David Atwood, for his unconditional love, support, and encouragement to follow my dreams, as well as his willingness to follow me wherever our path takes us. I owe so much of my success to my family, and especially my mother, Helen Caissie, and father, Jeff Richbourg, for their unending support, helping me in my struggles, and of course, financially (promise I'll have a job one day). My furry family has provided more joy and laughter than what is probably normal, but so much of my sanity is owed to my mutt dog, Gio, and my horse, Pixie.

I am forever grateful to my mentor and friend, Dr. Margaret McNulty. My success thus far in science, my re-ignited passion for research, and my future are largely thanks to you and your trust in me. You have taught me how to be a better scientist, colleague, and horse-owner. Thank you for allowing me to learn in my own way, providing guidance when necessary, and encouragement throughout.

To my committee members, Dr. Tammy Dugas, Dr. Frank Andrews, Dr. Colin Mitchell, and Dr. Michelle Osborn, thank you for your time and dedication to my studies. Your support, constructive criticism, advice, and assistance is greatly appreciated, and has helped me significantly. Dr. Joseph Skillen, thank you for being the best Dean's Representative that any graduate student could ask for. You went above and beyond what is typically expected from your position, and I am most grateful.

I owe a big thanks to all of my friends I made during my program that provided necessary distractions, emotional support, and hours of judgement-free listening for me to vent: Emma Schachner, Carmen Arsuaga, Samia OBryan, Sofia Raldiris, Catherine Ta, Holly Attuso, Daria Coleridge, Carmel Fargason, and many others.

TABLE OF CONTENTS

ACKNOWLEDGEMENTS	ii
LIST OF FIGURES	v
ABSTRACT	vi
CHAPTER 1. INTRODUCTION	1
1.1 Review of Bone Biology	1
1.1.1 General Bone Biology	1
1.1.2 Bone Development	3
1.1.3 Bone Remodeling	4
1.2 Overview of Bone Diseases	6
1.2.1 Diseases of Bone Development	6
1.2.2 Diseases of Bone Remodeling	7
1.3 Bisphosphonate Treatments for Bone Diseases	8
1.4 Assessments of Bone Health	11
1.4.1 Non-Invasive Assessments	11
1.4.2 Invasive Assessments	14
1.4.2.1 Histology	14
1.4.2.2 Micro-Computed Tomography	16
1.4.3 Use of Imaging in Education and Research	16
1.5 Animal Models of Orthopedic Disease	17
1.5.1 Selection of Animal Models	17
1.5.2 Small Animal Models	19
1.5.3 Large Animal Models	19
1.6 Summary and Specific Aims.....	20
1.7 References	23
CHAPTER 2. INFLUENCE OF TILUDRONATE ON BONE CELLS, MORPHOLOGY AND REMODELING IN YOUNG HORSES	32
2.1 Introduction	32
2.2 Materials and Methods	34
2.3 Results	42
2.4 Discussion	49
2.5 References	56
CHAPTER 3. INFLUENCE OF CLODRONATE ON BONE CELLS, MORPHOLOGY, REMODELING AND HEALING IN YOUNG HORSES	59
3.1 Introduction	59
3.2 Materials and Methods	61
3.3 Results	66
3.4 Discussion	69
3.5 Reference.....	74

CHAPTER 4. ANATOMICAL VARIATION OF THE TARSUS IN COMMON	
INBRED MOUSE STRAINS	77
4.1 Introduction	77
4.2 Materials and Methods.....	79
4.3 Results	82
4.4 Discussion	85
4.5 References	92
CHAPTER 5. CONCLUDING REMARKS	96
5.1 Overall Summary of Findings	96
5.2 Significance of Research	97
5.3 Future Directions	99
5.4 References	99
APPENDICES	101
Appendix A: First Author Consent	101
Appendix B: <i>Veterinary Surgery</i> Consent	102
Appendix C: <i>Anatomical Record</i> Consent	103
VITA	104

LIST OF FIGURES

Figure 2.1 Tiludronate study design schematic	35
Figure 2.2 Bone biopsy from the tuber coxae	38
Figure 2.3 Labeled histological sections of bone biopsies	41
Figure 2.4 Representative Day 0 bone biopsies	43
Figure 2.5 Summary data of bone structure and remodeling parameters	44
Figure 2.6 Mean histological bone biopsy scores	45
Figure 2.7 Histologic images of cartilage foci	47
Figure 2.8 Histologic images from juvenile horse	48
Figure 3.1 Clodronate study design schematic	62
Figure 3.2 Schematic of statistical comparisons	67
Figure 3.3 Summary data of bone structure and remodeling parameters	70
Figure 4.1 Characteristics for study samples utilized	81
Figure 4.2 Representative 3D reconstructions of the left tarsus	84
Figure 4.3 Three-dimensional reconstructions of the left pes	85
Figure 4.4 Representative slices from microCT scans	86
Figure 4.5 Three-dimensional reconstructions for comparative anatomy	87
Figure 4.6 Decalcified H&E stained histologic sagittal sections	88

ABSTRACT

The use of advanced imaging techniques has greatly improved orthopedic research and education. Histology of bone is a method of evaluating bone morphology, bony cells, and bone remodeling in two-dimensions, while micro-computed tomography (microCT) is a three-dimensional analysis of bone morphology. Combined, these methods assist in providing a comprehensive analysis of bone. In this dissertation, these techniques were utilized to answer questions currently outstanding in veterinary medicine: the effect of bisphosphonates on equine bone, and variation in murine tarsal anatomy.

Bisphosphonates are drugs that reduce osteoclast-mediated bone resorption and have recently been approved for the use in horses. Despite prolific clinical use, there has been little evidence of their effect on bone in horses. Therefore, the goal of these studies was to determine the impact of bisphosphonates on bone in normal, young horses. This was accomplished by evaluating bone biopsies taken before and 60 days after a single bisphosphonate administration. Biopsies were analyzed using microCT and histomorphometry. We found that the bisphosphonates studied have minimal to no effect on bone morphology and remodeling, and therefore conclude that these drugs do not negatively impact bone, and have no effect after 60 days.

Mice are the most commonly utilized animal model for orthopedic research, and knowledge of normal anatomy is critical to identify pathologies secondary to disease. We found conflicting evidence regarding the tarsal anatomy in the mouse. While normal tarsal variation exists in other species, this has not been documented in the mouse.

Therefore, the purpose of this study was to characterize the tarsal anatomy of the mouse. MicroCT data from muroid tarsi were collected, and representative tarsi were evaluated by histology. Fusion of the central and tarsal bone III was present in all laboratory mice evaluated, but was not present in the laboratory rat or wild white-footed mouse. This fusion was confirmed via histology; however, hyaline cartilage was present, surrounded by mature trabecular bone indicating a joint remnant despite the fused state of the bones. We conclude that in certain laboratory mouse strains, the central and tarsal bone III are fused into a single bone.

CHAPTER 1.

INTRODUCTION

1.1 Review of Bone Biology

1.1.1 General Bone Anatomy

The normal human skeleton consists of 213 bones, which can be characterized based on shape and development (Clarke, 2008). These bones articulate together to provide a variety of functions to the body: structure and support to permit movement, storage of calcium and phosphate to maintain mineral homeostasis, and protection of internal organs and tissues (Weiner et al., 1999). General bone categories based on shape include long bones (e.g., femora, radii, and metacarpals), short bones (e.g., carpal and tarsal bones), flat bones (e.g., calvaria and ribs), and irregular bones (e.g., vertebrae) (Clarke, 2008). Long bones are longer than they are wide, comprised of a long, hollow shaft called the diaphysis, a rounded end proximal and distal to the growth plates called the epiphyses, and the area comprised of the growth plate between the diaphysis and epiphysis called metaphyses (Clarke, 2008). Contained within the diaphysis is a cavity called the medullary canal (Gray, 1918). Bone marrow is located within the bone medullary canal, and stores important hematopoietic and mesenchymal stem cells (Gurkan and Akkus, 2008). Short bones are as long as they are wide, and are composed of an outer cortical bone layer, with an inner trabecular bone center (Clarke, 2008). Flat bones are broad and thin, while irregular bones do not fit into the other categories and usually have unproportioned dimensions. However, they both contain an inner trabecular layer between dense cortical bone layers on either side (Gray and Goss, 1878, Rho et al., 1998).

Bone is an organ, comprised of a hierarchical network of mineralized collagen fibrils, carbonated apatite crystals, and water (Weiner and Wagner, 1998). There are two types of bone based on gross morphology of the tissue: cortical and trabecular. Cortical bone, or compact bone, is dense and solid, providing strength and structure to bones by surrounding the medullary cavities (Clarke, 2008). Cortical bone is arranged in osteons, which are comprised of cylindrical rings of collagen fibers called lamellae, and contain a central canal that houses a neurovascular bundle (McGavin and Zachary, 2006). Trabecular bone, or cancellous bone, is made up of hemi-osteons and are arranged in inter-connecting rods and plates, called trabeculae. This arrangement is directly related to the direction of stress placed on the particular bone.

The 3 main bone cells are osteoblasts, osteocytes, and osteoclasts (Raggatt and Partridge, 2010). Osteoblasts are derived from pluripotent mesenchymal stem cells, and are the bone-forming cells that synthesize the organic matrix and promote mineralization. Osteocytes are osteoblasts that become encapsulated within lacunae in newly-formed bone. Osteocytes have long processes that extend through small tunnels throughout the bone extracellular matrix. These small tunnels, or canaliculi, permit communication between osteocytes, as well as the bone surface (Raggatt and Partridge, 2010). Osteoclasts are macrophage polykaryons, formed through the differentiation of monocyte precursor cells, that degrades bone matrix by secreting enzymes and acid (Boyle et al., 2003).

1.1.2 Bone Development

There are two classifications of bone development: endochondral and intramembranous ossification. Endochondral ossification is the process where bone replaces pre-existing cartilaginous anlagen (Olsen et al., 2000). The cartilaginous templates are formed during embryogenesis when mesenchymal cells condense and differentiate into chondrocytes (Erlebacher et al., 1995). After formation, chondrocytes within the anlagen proliferate and expand, producing cartilage matrix. Centrally-located chondrocytes mature into hypertrophic chondrocytes, creating a sequence of events that triggers specific factors to induce angiogenesis. During angiogenesis, osteoblasts, osteoclasts, and hematopoietic cells are brought into the location, allowing for mineralization to occur and creating primary ossification centers (Olsen et al., 2000). Endochondral ossification accounts for the formation of most of the skeleton, including the appendicular and axial skeleton (Ortega et al., 2004).

Intramembranous ossification is the process by which mesenchymal cells differentiate directly into osteoblast cells, which produce bone directly without a cartilaginous precursor. Briefly, ossification begins with a thin layer of mesenchymal cells. As these cells become highly vascularized, they differentiate into isolated osteoblasts, which begin to secrete osteoid. This osteoid matrix will become mineralized by the end of the embryonic period, forming the beginning of the osteon (Cooper et al., 2006). Flat bones of the skull and addition of new bone along the surfaces of long bones form through this process (Erlebacher et al., 1995).

1.1.3 Bone Remodeling

Bones undergo normal remodeling in order to maintain structure and integrity, repair damage in response to external and internal forces, and maintain homeostasis of minerals within the body. Overall, there are five phases of bone remodeling: activation, resorption, reversal, formation, and termination (Raggatt and Partridge, 2010). However, the completion of these events may vary greatly due to pathology or pharmacological treatments (Eriksen, 2010). During the activation phase, signals to initiate the remodeling process are detected by osteocytes (Bonewald, 2007), which can be due to structural damage or hormonal changes (Raggatt and Partridge, 2010), such as changes in estrogen or PTH (Eriksen, 2010). Osteocytes play an important role in detecting structural stresses and translating them into bone remodeling activation signals (Aarden et al., 1994). Osteocytes secrete transforming growth factor β (TGF- β) under normal conditions, which inhibits osteoclastogenesis and slows down overall remodeling rates; however, when bone is under stress, osteocytes undergo apoptosis which increases osteoclastogenesis (Aguirre et al., 2006). The resorption phase follows activation, where osteoblasts respond to the signals produced by the osteocytes, and recruit osteoclast precursors to the area of remodeling activity. Additionally, osteoblasts produce a chemoattractant that recruits osteoclast precursors and receptor activators of NF- κ B ligand (RANKL), which promotes osteoclastogenesis (Li et al., 2007). Osteoblasts also secrete matrix metalloproteinases (MMPs) that break down the lining of the bone surface and expose adhesion sites necessary for osteoclast attachment (Raggatt and Partridge, 2010). Osteoclasts attach themselves to the bone matrix, and rearrange their cytoskeleton so that a dense, actin structure forms a tight seal along the

edges of the osteoclast (Lakkakorpi et al., 1989). These edges enlarge and form a ruffled border (Stenbeck, 2002), completing the seal, and allowing the osteoclast to create a micro-environment within the sealed area under the osteoclast, which is critical in bone resorption (Baron, 1989). Once attached, osteoclasts create an acidic microenvironment by use of hydrogen pumps. Together with other enzymes, this degrades the bone matrix beneath the osteoclast, creating a Howship's lacuna (Teitelbaum, 2000). Following resorption, the reversal phase begins, where mononuclear cells of undetermined lineage prepare the bone surface for bone formation by removing collagen remnants and producing bone formation signals (Raggatt and Partridge, 2010). Factors that initiate the formation phase from reversal phase have not been fully identified, but include a coupling factor that promotes bone formation while inhibiting bone resorption (Martin and Sims, 2005). Mesenchymal stem cells or osteoblast progenitor cells are directed to the lacunae to differentiate and produce osteoid. After deposition, hydroxyapatite is incorporated into the newly formed osteoid, finalizing the bone formation (Raggatt and Partridge, 2010). Finally, the termination phase begins when the resorbed bone has been replaced, which is thought to be induced by a lack of sclerostin expression that was present during bone formation phases (Sapir-Koren and Livshits, 2014). The resting bone surface is reestablished, and continues in this state until the remodeling process begins again (Raggatt and Partridge, 2010).

1.2 Overview of Bone Diseases

1.2.1 Diseases of Bone Development

Due to the complex nature of bone formation, it should follow that any slight disturbance in these coordinated events can result in skeletal pathologies. During endochondral bone development, there are numerous factors that control specific processes necessary for normal bone development. During chondrogenesis, Sox proteins (e.g., Sox9) are critical for differentiation of mesenchymal stem cells into chondrocytes (Akiyama et al., 2002), proliferation of chondrocytes in growth plates of long bones (Akiyama et al., 2004), and upregulation of gene expression responsible for producing critical components of cartilaginous matrix (Bi et al., 2001). Additionally, fibroblast growth factor receptor (FGFR) 3 is expressed in proliferating chondrocytes (Provot and Schipani, 2005). FGFR3 affects long bone development and specific mutations within it cause skeletal dysplasias including achondroplasia, hypochondroplasia, and thanatophoric dysplasia, which are all forms of short-limb dwarfism (Vajo et al., 2000, Ornitz and Marie, 2002). Bone morphogenetic proteins (BMPs) are vital to inducing cartilage and bone formation. During development, BMP signaling is critical during the formation of joints by stimulating cartilage formation, localizing the expression of joint molecular markers to the appropriate location, and causing apoptosis at the joint location to create the cavitation (Baur et al., 2000, Yi et al., 2000). Inhibition of BMP signals can result in brachypodism (Storm et al., 1994), where the appendicular skeleton is affected and characterized by shorter phalanges with irregular ossification patterns (Grüneberg and Lee, 1973). These abnormalities occur before the formation of the cartilage anlagen and, being an abnormality of the

blastemata, result in abnormal fusions of the carpal and tarsal bones (e.g., fusion of the navicular and tarsal bone III in the tarsus) (Grüneberg and Lee, 1973).

1.2.2 Diseases of Bone Remodeling

In order for bone to remain structurally sound and functional, there must be a balance of bone formation and resorption, resulting in minimal to no net changes in the amount of bone in a healthy, mature skeleton. However, this delicate balance can be disrupted by certain pathologies which can affect both bone forming and bone resorbing pathways. Osteoporosis is one of the most common forms of bone remodeling disorders, where there is an overall loss in bone mass, causing bone fragility (Feng and McDonald, 2011). Due to the broad nature of this disease, it is divided into primary and secondary types (Panel, 2001, Marcus and Bouxsein, 2008). Primary osteoporosis is caused by age-related events, such as decreased gonadal activity (Riggs et al., 1969), while secondary osteoporosis is a consequence of chronic medical conditions that result in bone loss, such as cancer, hyperparathyroidism, use of corticosteroids, renal failure and vitamin D deficiency (Moyad, 2003, Painter et al., 2006). Age-related osteoporosis occurs most commonly due to the lack of gonadal function (Riggs et al., 1969), where there is a decrease in estrogen or testosterone. This leads to increased bone resorption that exceeds normal bone formation, resulting in a net loss of bone. However, osteoporosis does occur in both men and women, and can occur before age-related hormonal changes (Riggs et al., 1969, Painter et al., 2006). Hypogonadism can occur in young women and men, such as during androgen deprivation therapy for prostate carcinoma (Mittan et al., 2002) or anorexia (Grinspoon et al., 2000). Aside from sex

hormone changes, there are multiple factors that lead to an increase in parathyroid hormone (PTH) levels, such as primary hyperparathyroidism (Painter et al., 2006) or a decrease in calcium resorption in the gastrointestinal tract (Feng and McDonald, 2011), that result in increased bone resorption rate.

Bone remodeling disease in humans, such as with osteoporosis, affects the entire skeleton and is a systemic change in bone mass. In some animal species, however, bone disorders exist that affect only specific bones and do not result in a net change in the rest of the skeleton. In the horse, navicular disease is a degenerative disease of the navicular (distal sesamoid) bone within the hoof, along with its associated soft tissue structures (i.e., deep digital flexor tendon, impar ligament, and navicular bursa). Navicular disease is characterized by excessive remodeling of the navicular bone and a loss of bone mass (Widmer et al., 2000). The etiopathogenesis of navicular disease is complex and multifactorial, potentially including biomechanical (Wright and Douglas, 1993), vascular (Colles and Hickman, 1977, Doige and Hoffer, 1983) and hereditary components (Bos et al., 1986). Vascular changes include arteriosclerosis and thrombosis of the supplying arteries of the navicular bone (Colles and Hickman, 1977), while biomechanical changes in the load applied to the navicular bone can lead to damage and increased remodeling in response to the increased load (Trotter, 2001).

1.3 Bisphosphonate Treatments for Diseases of Bone Remodeling

Management of bone disease, including osteoporosis, was advanced greatly by the use of bisphosphonate drugs in the late 1960s (Russell, 2011). Bisphosphonates (BPs) are a chemically stable form of inorganic pyrophosphate, which gives BPs a

strong specific affinity for calcium, and are composed of two phosphonate groups. BPs are separated into two classes based on their chemical structure: nitrogen-containing BPs (e.g., zoledronate, alendronate, and ibandronate) and non-nitrogen containing BPs (e.g., clodronate, tiludronate, and etidronate) (Russell et al., 1999). Differences in individual bisphosphonate drugs within each class depend on the compound attached to the functional, or R-, group (Reszka and Rodan, 2003). Both classes, however, inhibit osteoclast-mediated bone loss by decreasing osteoclast activity. Nitrogen-containing BPs are more potent in reducing osteoclast-mediated bone loss than non-nitrogen-containing BPs, and changes in the functional group can also lead to different physiochemical and pharmacologic modifications. Non-nitrogen containing BPs have been shown to affect osteoclasts by disrupting intracellular metabolism through methylene-containing analogs of adenosine triphosphate (ATP) (Frith et al., 2001). This converts the BP into a toxic metabolite within the cell, and accumulation of this metabolite inhibits the mitochondrial adenine nucleotide translocase, resulting in the loss of the mitochondrial membrane potential (Lehenkari et al., 2002). These events lead to apoptosis of the osteoclast, ultimately inhibiting bone resorption (Reszka and Rodan, 2003). Nitrogen-containing BPs inhibit osteoclast activity by disrupting farnesyl diphosphate synthase (van Beek et al., 1999, Fisher et al., 2000), an enzyme in the mevalonate pathway, that stimulates isoprenylation, which is important in regulating osteoclast morphology, cytoskeletal arrangement, vesicular trafficking, and membrane ruffling (Zhang et al., 1995, Chellaiah et al., 2000). There appears to be a dose-dependent response of nitrogen-containing BPs, where small concentrations inhibit osteoclast functions necessary for bone resorption, and high concentrations lead to

osteoclast apoptosis (Halasy-Nagy et al., 2001). Therefore, nitrogen-containing BPs are exceptional inhibitors of bone resorption (Kimmel, 2007).

The pharmacokinetics of BPs depends on their classification (Licata, 2005). In general, BPs are polar compounds, making them poorly, yet rapidly absorbed after being ingested (Lin, 1996). BPs generally have <2% bioavailability (Yakatan et al., 1982), and have low plasma protein binding of approximately 30% (Pentikäinen et al., 1989). The peak serum concentration is obtained quickly following a single oral dose, within approximately 30 minutes (Laitinen et al., 2000). Most BPs are not metabolized, and are therefore excreted unchanged (Pentikäinen et al., 1989). BPs have a half-life of approximately two hours, with bone uptake and renal clearance accounting for the rapid clearance from plasma (Cocquyt et al., 1999). BPs have a high affinity for exposed hydroxyapatite, which occurs when bone surfaces are preparing for or currently undergoing bone resorption (Sato et al., 1991, Lin, 1996), which allows BPs to be taken up and stored in bone mineral surfaces (Russell et al., 1999), accounting for approximately 50-60% of the absorbed dose (Licata, 2005). The amount of BP released from bone depends on the rate of the remodeling process (Gatti and Adami, 1999), as the BPs are released when the bone matrix is dissolved during the remodeling process.

In addition to inhibiting bone resorption, the non-nitrogen containing BPs clodronate and etidronate have been shown to produce analgesic effects by entering neurons through the SLC20/34, and inhibiting glutamate and/or ATP transporters (Shima et al., 2016). Taken together, bisphosphonates are used in the treatment of numerous bone diseases in humans, including osteoporosis, Paget's disease, hypercalcemia of malignancies associate with myeloma and bone metastases, and

osteogenesis imperfecta (Russell, 2011), and recently for horses with navicular disease (Denoix et al., 2003, Whitfield et al., 2016) and other skeletal pathologies [e.g., osteoarticular disease (Coudry et al., 2007, Gough et al., 2010, Soto and Barbará, 2014) in veterinary medicine.

1.4 Assessments of Bone Health

1.4.1 Non-Invasive Assessments

In many bone diseases, diagnostic and assessment of disease progression are critical factors in minimizing negative outcomes for a patient. Historically, obtaining a bone biopsy was considered the most powerful and informative evaluation technique for bone assessment (Malluche et al., 1999). However, this method is invasive, and may not be desirable in a diseased patient. In a human clinical setting, obtaining informational data, while remaining as non-invasive as possible, is critical in patient care and disease management. Radiographic imaging has long been the gold standard for evaluating a variety of pathologies, including bone disease (van de Heijde, 2000). Radiographs are obtained by photons generated and emitted from a cathode tube that is collimated to a specific region of interest. As the photons pass through the body, the photons will be attenuated by tissue according to density, providing levels of exposure to film for imaging (Drake et al., 2014). Although radiographs are routinely used in numerous fields of medicine, they can only detect bone losses of greater than 40-50%, and are therefore not sensitive enough to monitor progression of disease or treatment (Moyad, 2003).

For diseases that lead to bone loss, the bone mineral density (BMD) measurement is the primary diagnostic test and is the gold standard and best predictor of fracture risk (Hui et al., 1989, Moyad, 2003). BMD produces a relative, overall T-score that describes the number of standard deviations a patient's density is from a group of similarly matched young, normal individuals. There are numerous ways to obtain BMD, including ultrasound, computerized tomography (Yakatan et al.), dual-energy X-ray absorptiometry (DEXA) and radiographs (Moyad, 2003). Ultrasound is the use of high frequency acoustic waves produced by piezoelectric material that passes through tissues without the use of ionizing radiation. As the waves pass, they bounce back based on tissue properties, are received back through the piezoelectric material, and are interpreted by a computer, producing a real-time image (Drake et al., 2014). Because it does not use radiation, ultrasound is a popular imaging modality, specifically in young adults and children, for monitoring bone disease (Siffert and Kaufman, 2007). In addition to providing information about bone density, ultrasound can also provide information about bone quality, such as elasticity and microarchitecture (Prins et al., 1997). However, there is little information about overall sensitivity and accuracy of serial measurements (Moyad, 2003). CT scans produce an image by passing a mobile X-ray tube around the body, creating a series of serially-sectioned two-dimensional images of the body (Drake et al., 2014). When these images are stacked together, a three-dimensional (3D) view is produced. CT is capable of producing extremely high-resolution images, but will emit increased radiation to do so. Therefore, although CT has the highest sensitivity in detecting changes in bone density and trabecular and cortical bone morphology, it is expensive, requires specialized software for analyses, and can

produce large amounts of radiation, making it challenging to obtain multiple scans over an extended period of time (Moyad, 2003). DEXA is a dual energy source of X-ray that has much higher sensitivity and accuracy, while also decreasing radiation exposure compared to other forms of radiation imaging. In addition, DEXA is inexpensive compared to other imaging modalities, making it an ideal technology for serial measurements, and is the current gold standard for obtaining BMD measurements in a clinical setting (Moyad, 2003).

In the veterinary clinical setting, the basic radiograph is still one of the most common diagnostic techniques utilized, but can be combined with additional imaging modalities, such as nuclear scintigraphy. Nuclear scintigraphy is a radionuclide bone imaging technique, where the uptake of radiopharmaceuticals, typically technetium-99m-labeled diphosphonates for bone, quickly deposits into the bone matrix (McKillop and Fogelman, 1984). Areas of increased uptake indicate areas of abnormal remodeling and mineralization. Nuclear scintigraphy is highly sensitive, making it possible to detect the earliest stages of bone disease; however, due to poor resolution, the specificity is generally moderate to low (Weller et al., 2001), and limits its use in bone imaging in both human and veterinary medicine. In systemic abnormal bone remodeling, specificity is not as important in diagnosis; however, in localized disease where small tissues are involved, such as navicular disease, specificity is crucial for accurate diagnosis and characterization. When combined with other imaging, such as radiography, nuclear scintigraphy is a more useful tool in diagnosing and monitoring abnormal bone remodeling (Weller et al., 2001), such as with navicular disease (Dyson, 2002) or osteochondral diseases (Kawcak et al., 2000).

1.4.2 Invasive Assessments

1.4.2.1 Histology

In research settings, there is less emphasis on patient comfort and longevity, and more emphasis on obtaining the most sensitive and accurate data possible, allowing for more invasive data collection methods. In this case, animal models of human disease are typically used, or animal models of animal disease in veterinary research. The more invasive technique of obtaining bone biopsies remains the gold standard for quantification of bone remodeling (Allen, 2003). Though obtaining bone biopsies is more invasive than most clinical settings prefer, research settings benefit greatly from numerous parameters available for direct evaluation through the use of histology. Histology is the process of embedding bone (or any other tissue) samples into a transparent material and taking thin, serial sections for examination under a microscope (Recker et al., 2011). Histomorphometry is the measurement of form and structure of a histologic tissue sample, permitting quantitative analysis of the structure (Duque and Watanabe, 2011). Previously, bone had to be de-mineralized by strong mineral or organic acids or acidic buffers, which would rapidly decalcify bone, so thin sections of bone could be sectioned for viewing (Recker et al., 2011). However, these agents were known to cause collagen fiber distortions and change the affinity of the tissue structure, weakening the staining outcomes; therefore, chelating agents, such as ethylenediamine tetraacetic acid (EDTA), have since replaced previous agents, as they do not have these negative secondary outcomes (Kiviranta et al., 1980). In the 1950s, however, a new method of embedding un-decalcified bone into plastic greatly improved bone research by allowing visualization and assessment of bone with its mineral components

(Frost et al., 1960). By preserving calcium in bone samples, a new technique of detecting newly-formed bone and mineralization, called fluorochrome labeling, was possible. Fluorochrome labeling uses injectable, calcium-binding tetracycline agents to directly measure bone remodeling dynamics *in vivo* over time (Frost, 1969). Tetracycline agents are able to make a complex with calcium that is deposited in areas of bone mineralization, and becomes permanently fixed within the mineralized matrix unless disturbed by subsequent remodeling processes (Frost et al., 1961). This deposition of tetracycline creates a brightly-lit area along the bone surface when exposed to ultra-violet light, indicating areas of remodeling and mineralization (Perrin, 1965). Fluorochrome bone labeling has since been greatly advanced, with new methods of labeling bone with up to 7 distinct labels analyzed by specialized spectral image acquisition software, allowing numerous time points for analyses with decreased tissue collection requirements (Pautke et al., 2005). In addition to bone remodeling, data on bone structure and bony cells are analyzed. Various staining solutions are utilized to highlight certain features, such as tartrate-resistant acidic phosphatase (TRAP) staining using an enzyme-histochemistry protocol for specific staining of osteoclasts and alkaline phosphatase (ALP) staining for osteoblasts. There are some limitations of histomorphometry, however. Overall, slicing sections of the sample is inherently destructive, and an analysis on a small portion of the skeleton is difficult to generalize to the rest of the skeleton. Additionally, histomorphometry is a 2D evaluation that determines 3D parameters through the mathematical discipline of stereology, which interpolates 3D measurements from 2D measurements using mathematical theorems. However, despite being an estimation of 3D parameters, there is minimal and

acceptable error when applied to trabecular bone from ilium samples (Parfitt et al., 1987, Dempster et al., 2013). Finally, histomorphometry is not the best assessment for bone mass, due to the 2D nature of the slice, as well as the small relative size of the section (Duque and Watanabe, 2011).

1.4.2.2 Micro-Computed Tomography

To overcome some limitations associated with histomorphometric analyses, evaluations are combined with micro-computed tomography (microCT). MicroCT is a high-resolution form of CT, and is an imaging modality to assess trabecular and cortical bone morphology with resolutions between 0.5 – 50 μm . MicroCT provides direct measurements of 3D bone morphology of entire biopsy samples, while providing excellent specificity and sensitivity using standardized parameters (Bouxsein et al., 2010). The high resolution increases radiation exposure to the sample; however, in research settings the specimens are usually taken from animals that are euthanized or biopsies are collected from live animals. Combined with histomorphometry, a comprehensive analysis is possible, obtaining information about bony cellular morphology, bone remodeling dynamics and bone structure (Duque and Watanabe, 2011).

1.4.3 Use of Imaging in Education and Research

With the advancements in medical imaging, anatomical education in both human and veterinary medicine have both benefited and incorporated many data in the medical anatomy curriculum. An in-depth understanding of anatomical structures and 3D

relationships is critical in medical training. High resolution images are obtained and can be combined to provide visual and technical experience for surgeons in training (Wiet et al., 2005). For example, high-resolution magnetic resonance imaging (MRI) and microCT data can be combined to visualize both soft and hard tissues within a sample, providing a visual and haptic display for a simulation of temporal bone dissection (Wiet et al., 2005). In addition to computerized visualizations, 3D printing is utilized in classrooms to provide additional understanding of anatomical structures (McMenamin et al., 2014). This is especially useful for biological structures or systems that are difficult to observe or manipulate in cadavers (AbouHashem et al., 2015). In addition to education, research relies on accurate representation of normal anatomical features, and benefit from high-resolution, 3D images of biological structures (Duce et al., 2010). Variation in reported anatomy greatly limits the potential for comparative anatomy between studies (Duce et al., 2010), and can limit the understanding of normal and pathological anatomical characteristics (El-Menyar et al., 2017).

1.5 Animal Models of Orthopedic Disease

1.5.1 Selection of Animal Models

Animal models play a crucial role in the understanding, prevention and treatment of orthopedic disease for both human and veterinary medicine. However, there are important distinctions between human and animal bone that have implications for research outcomes (Aerssens et al., 1998). For example, bone repair rates differ between large and small species, and are inversely related to the species' position on the phylogenetic scale, meaning rats have a higher rate of bone regeneration than

humans (Martini et al., 2001). In terms of bone composition, human bone is best represented by canine bone (Aerssens et al., 1998), but canine bone can withstand significantly higher compression strain than human bone (Kuhn et al., 1989). The use of quadrupeds as an animal model for human health has been questioned, especially in relation to differential loading secondary to bipedalism in humans. However, certain animal models can be selected based on specific criteria pertinent to the study (e.g., use of sheep in spine research due to similarities to humans in long axis loading (Smit, 2002)).

The type of animal model selected for research also depends on the aim of the study. When determining the pathogenesis and pathophysiology of a particular disease, smaller animals offer quick and cost-effective models than do larger animals. Small animal models also offer quick screenings of therapeutic interventions and drug safety. Large animal models, however, offer similar body size to humans and therefore can make therapeutic or surgical interventions more translatable to humans (Kuyinu et al., 2016). Thus, researchers must carefully evaluate the goals and anticipated outcomes of a study when determining the appropriate animal model. When evaluating animal diseases in veterinary medicine, researchers often have the benefit of using the specific animal of interest, eliminating the need for a translatable model. However, the disadvantages of the specific species have to be accounted for, including expense and the impact of ethical limitations imposed for use of companion animal species. Therefore, there is usually smaller sample sizes available for research utilizing large animal models.

1.5.2 Small Animal Models

The most common small animal orthopedic models include the rat, mouse, guinea pig and rabbit (Aerssens et al., 1998, Kuyinu et al., 2016). Small animal models have numerous advantages, including ease of handling, economical housing costs, short breeding cycles and well known genetics (Histing et al., 2011). For mice, a known genome make them the perfect model for utilizing genetic manipulations to study molecular mechanisms. Due to an increase in use of rodents in research, specifically mice, much information is known about their physiology, and many experimental protocols and kits are designed for this species. This makes their use more standard and widely available for additional research, and make them more favorable than a large animal model that does not have the same available data (Histing et al., 2011).

1.5.3 Large Animal Models

Non-human primates offer valuable information to human medicine due to their very similar physiological and behavioral characteristics (Kuyinu et al., 2016). Although non-human primates are the most relevant in terms of mimicking human disease, they are extremely expensive and are associated with ethical concerns, in addition to the possible spread of infectious disease, making them a difficult option for many researchers (Reinwald and Burr, 2008). Therefore, cost-effective alternatives to non-human primates, such as ungulate and canine species, are practical, large animal model substitutes. Although more expensive in terms of management, large animal models are a necessity in certain research, such as osteoporosis and osteoarthritis research, due to their longer lifespan, similarities in osteonal remodeling and naturally-

occurring disease (Reinwald and Burr, 2008). Additionally, it is extremely important that the animal model develop the desired disease in a similar pathway, such as a loss of estrogen in an osteoporosis model, so that therapeutic interventions behave similarly in both the animal model and human. Dogs have long been considered the ideal alternative to the non-human primate, and have been one of the most studied large animal models for orthopedic research (Martini et al., 2001). However, the use of dogs poses a similar ethical concern as do non-human primates due to their companion status (Rollin, 2006), and the use of dogs has since decreased in research settings. Pigs have physiological similarities to humans, including sequential skeletal phases of development. Sheep are another alternative large animal model, and are being used more frequently in orthopedic research due to their ease of handling (Martini et al., 2001). Horses are mostly utilized in osteoarthritis research, as they have a similar risk to humans for developing naturally-occurring osteoarthritis secondary to trauma or as a result of age, as well as exercise-related osteochondral defects (McIlwraith et al., 2012). Additionally, they are large enough to use standard imaging modalities. All of these species are large and expensive, making management and handling more difficult than small animal models, which are important considerations when initiating research studies using these models (Gregory et al., 2012).

1.6 Summary and Specific Aims

Overall, bone is a highly complex, active structure that provides organisms with essential protection and support. Orthopedic research has been greatly advanced by imaging modalities, allowing researchers to visualize and evaluate bone health, bone

diseases and therapeutic interventions for both human and veterinary medicine. Combining evaluation techniques, such as histology and microCT, can overcome the disadvantages of each technique, and provide comprehensive detail of bone morphology and cellular structure. In addition, advanced imaging techniques can be used to provide anatomy depictions for both research and education. Based on this, the following research has been performed to address currently unknown information in veterinary medicine regarding bone health in horses and muroid species, and is summarized in the following aims:

Aim 1: Determine the effect of the bisphosphonates tiludronate on normal bone turnover, bone morphology and bony cells in skeletally immature horses via microCT and histomorphometry.

Summary: To test the effect of tiludronate on bone, biopsies from the tuber coxarum were taken from ten horses aged two - five years old. A baseline biopsy was collected at Day 0, and horses were then administered either tiludronate or saline. Horses were administered oxytetracycline as a fluorescent bone label at Day 47 and 57 for evaluation of bone remodeling. A second biopsy was collected at Day 60 from the contralateral tuber coxarum. Samples were fixed and scanned by microCT for evaluation of trabecular bone morphology. The biopsies were then prepared for decalcified and un-decalcified histology for evaluation of bony cells, bone morphology and bone remodeling following standard techniques and nomenclature. This aim will establish if tiludronate affects normal bone structure and remodeling in skeletally immature horses. The hypothesis is that tiludronate will reduce osteoclast numbers and

function, resulting in increased bone volume and decreased bone remodeling in young horses.

Aim 2: Determine the effect of clodronate on normal bone turnover, morphology and repair in skeletally immature horses via microCT and histomorphometry.

Summary: Aim 2 utilized the study design and techniques as outlined in Aim 1. In brief, biopsies were taken from nine horses aged two – four years old; a baseline biopsy (Day 0), a contralateral biopsy (Day 60), and a re-biopsy of the initial site (Day 60R), providing a biopsy after a bone defect. Clodronate or saline was administered immediately following Day 0 biopsy collection. Preparation and assessments were identical to Aim 1. Additionally, the Day 60R biopsy was scanned via microCT and then prepared for decalcified histology. This aim will first establish our equine model as an adequate model of bone repair. Subsequently, this aim will determine if clodronate impacts bone structure and repair in skeletally immature horses. The hypothesis is that clodronate will result in increased bone formation in an equine model of bone healing, as well as reduce osteoclast numbers and function, resulting in increased bone volume and decreased bone remodeling in young horses.

Aim 3: Characterize the anatomy of the mouse tarsus and clarify the presence and number of bones within this region in normal laboratory mice.

Summary: Bony anatomy of the tarsi from two strains of commonly used laboratory mice (i.e., C57/Bl6 and BalbC) were evaluated for bony anatomy characteristics via microCT. This anatomy was compared to selected outgroups,

including the closely-related laboratory rat (Sprague Dawley[®]) and the more distantly related wild white-footed mouse (*Peromyscus leucopus*). Representative mouse tarsi were selected for routine decalcified histology preparation, where serial, sagittal sections were taken through the mid-tarsus. The hypothesis is that normal laboratory mice have a fusion of the central and tarsal bone III, which is not present in other outgroup species evaluated.

1.7 References

- Aarden, E. M., P. J. Nijweide and E. H. Burger (1994). "Function of osteocytes in bone." J Cell Biochem **55**(3): 287-299.
- AbouHashem, Y., M. Dayal, S. Savanah and G. Štrkalj (2015). "The application of 3D printing in anatomy education." Med Educ Online **20**: 1-3.
- Aerssens, J., S. Boonen, G. Lowet and J. Dequeker (1998). "Interspecies differences in bone composition, density, and quality: Potential implications for in vivo bone research " Endocrinology **139**(2): 663-670.
- Aguirre, J. I., L. I. Plotkin, S. A. Stewart, R. S. Weinstein, A. M. Parfitt, S. C. Manolagas and T. Bellido (2006). "Osteocyte Apoptosis Is Induced by Weightlessness in Mice and Precedes Osteoclast Recruitment and Bone Loss." J Bone Min Res **21**(4): 605-615.
- Akiyama, H., M. C. Chaboissier, J. F. Martin, A. Schedl and B. de Crombrughe (2002). "The transcription factor Sox9 has essential roles in successive steps of the chondrocyte differentiation pathway and is required for expression of Sox5 and Sox6." Genes Dev **16**(21): 2813-2828.
- Akiyama, H., J. P. Lyons, Y. Mori-Akiyama, X. Yang, R. Zhang, Z. Zhang, J. M. Deng, M. M. Taketo, T. Nakamura, R. R. Behringer, P. D. McCrea and B. de Crombrughe (2004). "Interactions between Sox9 and beta-catenin control chondrocyte differentiation." Genes Dev **18**(9): 1072-1087.
- Allen, M. J. (2003). "Biochemical markers of bone metabolism in animals: uses and limitations." Vet Clin Path **32**(3): 101-113.
- Baron, R. (1989). "Molecular mechanisms of bone resorption by the osteoclast." Anat Rec **224**(2): 317-324.

- Baur, S. T., J. J. Mai and S. M. Dymecki (2000). "Combinatorial signaling through BMP receptor IB and GDF5: shaping of the distal mouse limb and the genetics of distal limb diversity." Development **127**(3): 605-619.
- Bi, W., W. Huang, D. J. Whitworth, J. M. Deng, Z. Zhang, R. R. Behringer and B. de Crombrughe (2001). "Haploinsufficiency of Sox9 results in defective cartilage primordia and premature skeletal mineralization." Proc Natl Acad Sci U S A **98**(12): 6698-6703.
- Bonewald, L. F. (2007). "Osteocytes as dynamic multifunctional cells." Ann N Y Acad Sci **1116**(1): 281-290.
- Bos, H., G. J. W. Meij and K. J. Dik (1986). "Heredity of navicular disease." Vet Quart **8**(1): 68-72.
- Bouxsein, M. L., S. K. Boyd, B. A. Christiansen, R. E. Guldberg, K. J. Jepsen and R. Müller (2010). "Guidelines for assessment of bone microstructure in rodents using micro-computed tomography." J Bone Min Res **25**(7): 1468-1486.
- Boyle, W. J., W. S. Simonet and D. L. Lacey (2003). "Osteoclast differentiation and activation." Nature **423**: 337-342.
- Chellaiah, M. A., N. Soga, S. Swanson, S. McAllister, U. Alvarez, D. Wang, S. F. Dowdy and K. A. Hruska (2000). "Rho-A is critical for osteoclast podosome organization, motility, and bone resorption." J Biol Chem **275**(16): 11993-12002.
- Clarke, B. (2008). "Normal bone anatomy and physiology." Clin J Am Soc Nephrol **3**(Supplement 3): S131-S139.
- Cocquyt, V., W. F. Kline and B. J. Gertz (1999). "Pharmacokinetics of Intravenous Alendronate." J Clin Pharmacol **39**: 385-393.
- Colles, C. M. and J. Hickman (1977). "The arterial supply of the navicular bone and its variations in navicular disease." Equine Veterinary Journal **9**(3): 150-154.
- Colles, C. M. and J. Hickman (1977). "The arterial supply of the navicular bone and its variations in navicular disease." Equine Vet J **9**(3): 150-154.
- Cooper, C., S. Westlake, N. Harvey, K. Javaid, E. Dennison and M. Hanson (2006). "Review: developmental origins of osteoporotic fracture." Osteoporos Int **17**(3): 337-347.
- Coudry, V., D. Thibaud, B. Riccio, F. Audigié, D. Didierlaurent and J.-M. Denoix (2007). "Efficacy of tiludronate in the treatment of horses with signs of pain associated with osteoarthritic lesions of the thoracolumbar vertebral column." Am J Vet Res **68**(3): 329-337.

- Dempster, D. W., J. E. Compston, M. K. Drezner, F. H. Glorieux, J. A. Kanis, H. Malluche, P. J. Meunier, S. M. Ott, R. R. Recker and A. M. Parfitt (2013). "Standardized nomenclature, symbols, and units for bone histomorphometry: a 2012 update of the report of the ASBMR Histomorphometry Nomenclature committee." J Bone Miner Res **28**(1): 1-16.
- Denoix, J. M., D. Thibaud and B. Riccio (2003). "Tiludronate as a new therapeutic agent in the treatment of navicular disease: a double-blind placebo-controlled clinical trial." Equine Vet J **34**(4): 407-413.
- Doige, C. E. and M. A. Hoffer (1983). "Pathological changes in the navicular bone and associated structures of the horse." Can J Comp Med **47**: 387-395.
- Drake, R., A. W. Vogl and A. Mitchell (2014). Gray's Anatomy for Students, Churchill Livingstone.
- Duce, S., L. Madrigal, K. Schmidt, C. Cunningham, G. Liu, S. Barker, G. Tennant, C. Tickle, S. Chudek and Z. Miedzybrodzka (2010). "Micro-magnetic resonance imaging and embryological analysis of wild-type and pma mutant mice with clubfoot." J Anat **216**(1): 108-120.
- Duque, G. and K. Watanabe, Eds. (2011). Osteoporosis Research: Animal Models, Springer Science & Business Media.
- Dyson, S. J. (2002). "Subjective and quantitative scintigraphic assessment of the equine foot and its relationship with foot pain." Equine Vet J **34**(2): 164-170.
- El-Menyar, A., M. Asim, G. Jabbour and H. Al-Thani (2017). "Clinical implications of the anatomical variation of deep venous thrombosis." Phlebology.
- Eriksen, E. F. (2010). "Cellular mechanisms of bone remodeling." Rev Endocr Metab Disord **11**(4): 219-227.
- Erlebacher, A., E. H. Filvaroff, S. E. Gitelman and R. Derynck (1995). "Toward a molecular understanding of skeletal development." Cell **80**: 371-378.
- Feng, X. and J. M. McDonald (2011). "Disorders of bone remodeling." Annu Rev Pathol **6**: 121-145.
- Fisher, J. E., G. A. Rodan and A. A. Reszka (2000). "In vivo effects of bisphosphonates on the osteoclast mevalonate pathway." Endocrinology **141**(12): 4793-4796.
- Frith, J. C., J. Mönkkönen, S. Auriola, H. Mönkkönen and M. J. Rogers (2001). "The molecular mechanism of action of the antiresorptive and antiinflammatory drug clodronate: evidence for the formation in vivo of a metabolite that inhibits bone resorption and causes osteoclast and macrophage apoptosis." Arthritis Rheum **44**(9): 2201-2210.

- Frost, H. M. (1969). "Tetracycline-based histological analysis of bone remodeling." Calcif Tissue Int **3**: 211-237.
- Frost, H. M., A. R. Villanueva and H. Roth (1960). "Measurement of bone formation in a 57 year old man by means of tetracyclines." Henry Ford Hosp Med Bull **8**: 239-254.
- Frost, H. M., A. R. Villanueva, H. Roth and S. Stanisavljevic (1961). "Tetracycline bone labeling." J New Drugs **1**(5): 206-216.
- Gatti, D. and S. Adami (1999). "New bisphosphonates in the treatment of bone diseases." Drugs Aging(15): 4.
- Gough, M. R., D. Thibaud and R. K. W. Smith (2010). "Tiludronate infusion in the treatment of bone spavin: a double blind placebo-controlled trial." Equine Vet J **42**(5): 381-387.
- Gray, H. (1918). Anatomy of the Human Body, Lea & Febiger.
- Gray, H. and C. M. Goss (1878). Anatomy of the Human Body, Lea & Febiger.
- Gregory, M. H., N. Capito, K. Kuroki and A. M. Stoker (2012). "A review of translational animal models for knee osteoarthritis." Arthritis **2012**: 14.
- Grinspoon, S., E. Thomas, S. Pitts, E. Gross, D. Mickley, K. Miller, D. Herzog and A. Klibanski (2000). "Prevalence and predictive factors for regional osteopenia in women with anorexia nervosa." Ann Intern Med **133**(10): 790-794.
- Grüneberg, H. and A. J. Lee (1973). "The anatomy and development of brachypodism in the mouse." J Embryol Exp Morphol **30**(1): 119-141.
- Gurkan, U. A. and O. Akkus (2008). "The mechanical environment of bone marrow: a review." Annals of biomedical engineering **36**(12): 1978-1991.
- Halasy-Nagy, J., G. Rodan and A. Reszka (2001). "Inhibition of bone resorption by alendronate and risedronate does not require osteoclast apoptosis." Bone **29**(6): 553-559.
- Histing, T., P. Garcia, J. H. Holstein, M. Klein, R. Matthys, R. Nuetzi, R. Steck, M. W. Laschke, T. Wehner, R. Bindl, S. Recknagel, E. K. Stuermer, B. Vollmar, B. Wildemann, J. Lienau, B. Willie, A. Peters, A. Ignatius, T. Pohlemann, L. Claes and M. D. Menger (2011). "Small animal bone healing models: standards, tips, and pitfalls results of a consensus meeting." Bone **49**: 591-599.
- Hui, S. L., C. W. Slemenda and C. C. Johnston, Jr. (1989). "Baseline measurement of bone mass predicts fracture in white women." Ann Intern Med **111**(5): 355-361.

- Kawcak, C. E., C. W. McIlwraith, R. W. Norrдин, P. D. Park and P. S. Steyn (2000). "Clinical effects of exercise on subchondral bone of carpal and metacarpophalangeal joints in horses." Am J Vet Res **61**(10).
- Kimmel, D. B. (2007). "Mechanism of action, pharmacokinetic and pharmacodynamic profile, and clinical applications of nitrogen-containing bisphosphonates." J Dent Res **86**(11): 1022-1033.
- Kiviranta, I., M. Tammi, R. Lappalainen and T. Kuusela (1980). "The rate of calcium extraction during EDTA decalcification from thin bone slices as assessed with atomic absorption spectrophotometry." Histochemistry **68**(2): 119-127.
- Kuhn, J. L., S. A. Goldstein, M. J. Ciarelli and L. S. Matthews (1989). "The limitations of canine trabecular bone as a model for human: a biomechanical study." J Biomech **22**(2): 95-107.
- Kuyinu, E. L., G. Narayanan, L. S. Nair and C. T. Laurencin (2016). "Animal models of osteoarthritis: classification, update, and measurement of outcomes." J Orthop Surg Res **11**: 19.
- Laitinen, K., A. Patronen, P. Harju and E. Löyttyniemi (2000). "Timing of food intake has a marked effect on the bioavailability of clodronate." Bone **27**(2): 293-296.
- Lakkakorpi, P., J. Tuukkanen, T. Hentunen, K. Järvelin and K. Väänänen (1989). "Organization of osteoclast microfilaments during the attachment to bone surface in vitro." J Bone Miner Res **4**(6): 817-825.
- Lehenkari, P. P., M. Kellinsalmi, J. P. Näpänkangas, K. V. Ylitalo, J. Mönkkönen, M. J. Rogers, A. Azhayev, K. H. Väänänen and I. E. Hassinen (2002). "Further insight into mechanism of action of clodronate: inhibition of mitochondrial ADP/ATP translocase by a nonhydrolyzable, adenine-containing metabolite." Mol Pharmacol **61**(5): 1255-1262.
- Li, X., M. Bergenstock, L. M. Bevelock, D. V. Novack and N. C. Partridge (2007). "Parathyroid hormone stimulates osteoblastic expression of MCP-1 to recruit and increase the fusion of pre/osteoclasts." J Biol Chem **282**(45): 33098-33106.
- Licata, A. A. (2005). "Discovery, clinical development, and therapeutic uses of bisphosphonates." Ann Pharmacother **39**: 668-677.
- Lin, J. H. (1996). "Bisphosphonates: a review of their pharmacokinetic properties." Bone **18**(2): 75-85.
- Malluche, H. H., M. C. Langub and M. C. Monier-Faugere (1999). "The role of bone biopsy in clinical practice and research." Kidney Int **56**(S 73): S-20 - S-25.
- Marcus, R. and M. Bouxsein (2008). The nature of osteoporosis. San Diego, Academic.

- Martin, T. J. and N. A. Sims (2005). "Osteoclast-derived activity in the coupling of bone formation to resorption." Trends Mol Med **11**(2): 76-81.
- Martini, L., M. Fini, G. Giavaresi and R. Giardino (2001). "Sheep model in orthopedic research: a literature review." Comp Med **51**(4): 292-299.
- McGavin, M. D. and J. F. Zachary (2006). Pathologic Basis of Veterinary Disease, Elsevier Health Sciences.
- McIlwraith, C., D. Frisbie and C. Kawcak (2012). "The horse as a model of naturally occurring osteoarthritis." Bone Joint Res **1**(11): 297-309.
- McKillop, J. H. and I. Fogelman (1984). "Bone scintigraphy in benign bone disease." BMJ **288**: 264-266.
- McMenamin, P. G., M. R. Quayle, C. R. McHenry and J. W. Adams (2014). "The production of anatomical teaching resources using three-dimensional (3D) printing technology." Anat Sci Educ **7**(6): 479-486.
- Mittan, D., S. Lee, E. Miller, R. C. Perez, J. W. Basler and J. M. Bruder (2002). "Bone loss following hypogonadism in men with prostate cancer treated with GnRH analogs." J Clin Endocrinol Metab **87**(8): 3656-3661.
- Moyad, M. A. (2003). "Osteoporosis: a rapid review of risk factors and screening methods." Urol Oncol **21**: 375-379.
- Olsen, B. R., A. M. Reginato and W. Wang (2000). "Bone development." Annu Rev Cell Dev Biol **16**: 191-220.
- Ornitz, D. M. and P. J. Marie (2002). "FGF signaling pathways in endochondral and intramembranous bone development and human genetic disease." Genes Dev **16**(12): 1446-1465.
- Ortega, N., D. J. Behonick and Z. Werb (2004). "Matrix remodeling during endochondral ossification." Trends Cell Biol **14**(2): 86-93.
- Painter, S. E., M. Kleerekoper and P. M. Camacho (2006). "Secondary osteoporosis: a review of the recent evidence." Endocr Pract **12**(4): 436-445.
- Panel, N. I. H. C. D. (2001). "Osteoporosis prevention, diagnosis, and therapy." JAMA **285**(6): 785-795.
- Parfitt, A. M., M. K. Drezner, F. H. Glorieux, J. A. Kanis, H. Malluche, P. J. Meunier, S. M. Ott and R. R. Recker (1987). "Bone histomorphometry: standardization of nomenclature, symbols, and units: report of the ASBMR Histomorphometry Nomenclature Committee." J Bone Miner Res **2**(6): 595-610.

- Pautke, C., S. Vogt, T. Tischer, G. Wexel, H. Deppe, S. Milz, M. Schieker and A. Kolk (2005). "Polychrome labeling of bone with seven different fluorochromes: enhancing fluorochrome discrimination by spectral image analysis." Bone **37**(4): 441-445.
- Pentikäinen, P., I. Elomaa, A. Nurmi and S. Kärkkäinen (1989). "Pharmacokinetics of clodronate in patients with metastatic breast cancer." Int J Clin Pharmacol Ther Toxicol **27**(5): 222-228.
- Perrin, D. D. (1965). "Binding of tetracyclines to bone." Binding of tetracyclines to bone **208**: 787-788.
- Prins, S. H., H. L. Jorgensen, L. V. Jorgensen and C. Hassager (1997). "The role of quantitative ultrasound in the assessment of bone: a review." Clin Physiol **18**(1): 3-17.
- Provot, S. and E. Schipani (2005). "Molecular mechanisms of endochondral bone development." Biochem Biophys Res Commun **328**: 658-665.
- Raggatt, L. J. and N. C. Partridge (2010). "Cellular and molecular mechanisms of bone remodeling." J Biol Chem **285**(33): 25103-25108.
- Recker, R. R., D. B. Kimmel, D. Dempster, R. S. Weinstein, T. J. Wronski and D. B. Burr (2011). "Issues in modern bone histomorphometry." Bone **49**(5): 955-964.
- Reinwald, S. and D. Burr (2008). "Review of nonprimate, large animal models for osteoporosis research." J Bone Miner Res **23**(9): 1353-1368.
- Reszka, A. A. and G. A. Rodan (2003). "Mechanism of action of bisphosphonates." Curr Osteoporos Rep **1**(2): 45-52.
- Rho, J. Y., L. Kuhn-Spearing and P. Zioupos (1998). "Mechanical Properties and the Hierarchical Structure of Bone." Med Eng Phys **20**: 92-102.
- Riggs, B. L., J. Jowsey, P. J. Kelly and J. D. Jones (1969). "Effect of sex hormones on bone in primary osteoporosis." J Clin Invest **48**: 1065-1072.
- Rollin, B. E. (2006). "The regulation of animal research and the emergence of animal ethics: a conceptual history." Theor Med Bioeth **27**: 285-304.
- Russell, G. R. G. (2011). "Bisphosphonates: The first 40years." Bone **49**(1): 2-19.
- Russell, G. R. G., M. J. Rogers, J. C. Frith, S. P. Luckman, F. P. Coxon, H. L. Benford, P. I. Croucher, C. Shipman and H. A. Fleisch (1999). "The pharmacology of bisphosphonates and new insights into their mechanisms of action." J Bone Miner Res **14**(S2): 53-65.

- Russell, R. G., P. I. Croucher and M. J. Rogers (1999). "Bisphosphonates: pharmacology, mechanisms of action and clinical uses." Osteoporos Int **9** (Suppl 2): S66-80.
- Sapir-Koren, R. and G. Livshits (2014). "Osteocyte control of bone remodeling: is sclerostin a key molecular coordinator of the balanced bone resorption–formation cycles?" Osteoporos Int **25**(12): 2685-2700.
- Sato, M., W. Grasser, N. Endo and R. Akins (1991). "Bisphosphonate action. Alendronate localization in rat bone and effects on osteoclast ultrastructure." J Clin Invest **88**(6): 2095-2105.
- Shima, K., W. Nemoto, M. Tsuchiya, K. Tan-No, T. Takano-Yamamoto, S. Sugawara and Y. Endo (2016). "The Bisphosphonates Clodronate and Etidronate Exert Analgesic Effects by Acting on Glutamate- and/or ATP-Related Pain Transmission Pathways." Biol Pharm Bull **39**(5): 770-777.
- Siffert, R. S. and J. J. Kaufman (2007). "Ultrasonic bone assessment: "The time has come"." Bone **40**(1): 5-8.
- Smit, T. H. (2002). "The use of a quadruped as an in vivo model for the study of the spine-biomechanical considerations." Eur Spine J **11**: 137-144.
- Soto, S. A. and A. C. Barbará (2014). "Bisphosphonates: pharmacology and clinical approach to their use in equine osteoarticular diseases." J Equine Vet Sci **34**: 727-737.
- Stenbeck, G. (2002). "Formation and function of the ruffled border in osteoclasts." Semin Cell Dev Biol **13**: 285-292.
- Storm, E. E., T. V. Huynh, N. G. Copeland, N. A. Jenkins, D. M. Kingsley and S. J. Lee (1994). "Limb alterations in brachypodism mice due to mutations in a new member of the TGF beta-superfamily." Nature **368**(6472): 639-643.
- Teitelbaum, S. L. (2000). "Bone resorption by osteoclasts." Science **289**(5484): 1504-1508.
- Trotter, G. (2001). "The Biomechanics of what Really Causes Navicular Disease." Equine Vet J **33**(4): 334-336.
- Vajo, Z., C. A. Francomano and D. J. Wilkin (2000). "The molecular and genetic basis of fibroblast growth factor receptor 3 disorders: the achondroplasia family of skeletal dysplasias, Muenke craniosynostosis, and Crouzon syndrome with acanthosis nigricans." Endocr Rev **21**(1): 23-39.
- van Beek, E., E. Pieterman, L. Cohen, C. Lowik and S. Papapoulos (1999). "Farnesyl pyrophosphate synthase is the molecular target of nitrogen-containing bisphosphonates." Biochem Biophys Res Commun **264**(1): 108-111.

- van de Heijde, D. M. F. M. (2000). "Radiographic imaging: the 'gold standard' for assessment of disease progression in rheumatoid arthritis." Rheumatology **39**(S 1): 9-16.
- Weiner, S., W. Traub and H. D. Wagner (1999). "Lamellar Bone: Structure–Function Relations." Journal of Structural Biology **126**(3): 241-255.
- Weiner, S. and H. D. Wagner (1998). "The material bone: structure-mechanical function relations." Annu Rev Mater Sci **28**(1): 271-298.
- Weller, R., L. Livesey, J. Maierl and K. Nuss (2001). "Comparison of radiography and scintigraphy in the diagnosis of dental disorders in the horse." Equine Vet J.
- Whitfield, C. T., M. J. Schoonover, T. C. Holbrook, M. E. Payton and K. M. Sippel (2016). "Quantitative assessment of two methods of tiludronate administration for the treatment of lameness caused by navicular syndrome in horses." Am J Vet Res **77**(2): 167-173.
- Widmer, W. R., K. A. Buckwalter, J. F. Fessler, M. A. Hill, D. C. VanSickle and S. Ivancevich (2000). "Use of radiography, computed tomography and magnetic resonance imaging for evaluation of navicular syndrome in the horse." Vet Radiol Ultrasound **41**(2): 108-116.
- Wiet, G. J., P. Schmalbrock, K. Powell and D. Stredney (2005). "Use of ultra-high-resolution data for temporal bone dissection simulation." Otolaryngol Head Neck Surg **133**: 911-915.
- Wright, I. and J. Douglas (1993). "Biomechanical considerations in the treatment of navicular disease." Vet Rec **133**(5): 109-114.
- Yakatan, G. J., W. J. Poynor, R. L. Talbert, B. F. Floyd, C. L. Slough, R. S. Ampulski and J. J. Benedict (1982). "Clodronate kinetics and bioavailability." Clin Pharmacol Ther **31**(4): 402-410.
- Yi, S. E., A. Daluiski, R. Pederson, V. Rosen and K. M. Lyons (2000). "The type I BMP receptor BMPRII is required for chondrogenesis in the mouse limb." Development **127**(3): 621-630.
- Zhang, D., N. Udagawa, I. Nakamura, H. Murakami, S. Saito, K. Yamasaki, Y. Shibasaki, N. Moril, S. Narumiya, N. Takahashi and T. Suda (1995). "The small GTP-binding protein, rho p21, is involved in bone resorption by regulating cytoskeletal organization in osteoclasts." J Cell Sci **108**: 2285-2292.

CHAPTER 2.

INFLUENCE OF TILUDRONATE ON BONE CELLS, MORPHOLOGY AND REMODELING IN YOUNG HORSES¹

2.1 Introduction

Tiludronate disodium (Tildren, Ceva Animal Health LLC, Lenexa, KS, USA) is a bisphosphonate drug that is licensed for use in horses to reduce lameness associated with navicular disease (Denoix et al., 2003, Whitfield et al., 2016). Tiludronate has a high affinity for bone (Henneman et al., 2008) and reduces osteoclastic activity (David et al., 1996), resulting in inhibition of bone resorption and subsequent uncoupling of the balanced remodeling process (Murakami et al., 1995, David et al., 1996, Kamm et al., 2008). Tiludronate has been shown to have potential effectiveness to treat musculoskeletal conditions other than navicular disease, such as distal tarsal joint osteoarthritis (Gough et al., 2010), thoracic and lumbar vertebral arthritis (Coudry et al., 2007) and dorsal metacarpal disease (Carpenter, 2012). However, these studies all report data on clinical outcomes (e.g., improvement in lameness), and not the effect on bone. Similarly, clinical studies have shown a reduction in lameness associated with navicular disease following tiludronate treatment (Denoix et al., 2003, Whitfield et al., 2016). One barrier to the field is currently a lack of data regarding the direct impact on bone remodeling kinetics in horses. Only a single study has attempted to evaluate tiludronate's direct impact on bone; however, it was unsuccessful (Delguste et al., 2007). In addition, tiludronate has been administered to young horses as a treatment for dorsal metacarpal disease (Carpenter, 2012), despite their still having to undergo a

¹ Parts of this chapter previously appeared as Mitchell, C.F. et al., Assessment of Tuber Coxae Bone Biopsy in the Standing Horse. *Vet Surg* (2017) DOI: 10.1111/vsu.12603. Reprinted by permission of John Wiley and Sons via RightsLink.

tremendous amount of bone remodeling as a part of normal bone growth (Müller et al., 1998). Despite the potential impact of tiludronate on normal bone remodeling kinetics, a detailed study has not been performed to determine if tiludronate negatively affects normal bone remodeling in young horses.

The gold standard for bone analyses are histomorphometry (Müller et al., 1998) and microCT (MacNeil and Boyd, 2007), both of which require bone biopsies. The tuber coxarum has been reported to be the easiest site for bone biopsy acquisition in the horse and is a region that was found to have consistently higher levels of tiludronate in comparison to other bones (Delguste et al., 2011). A recently published study by the authors has shown the tuber coxarum as a site to obtain reliable bony samples in a non-terminal equine model that are consistent in size and of adequate quality to evaluate trabecular bone using both histomorphometry and microCT (Mitchell et al., 2017).

Therefore, the aim of this study was to evaluate the effect of tiludronate on bony cells, bone morphology and remodeling in skeletally-immature, clinically healthy horses. This was accomplished by evaluating bone biopsies, obtained from the tuber coxarum using a previously published surgical technique (Mitchell et al., 2017), via microCT and histomorphometry. We hypothesized that tiludronate administration would result in increased bone volume, decreased osteoclast numbers and activity, and increased bone apposition when compared to control samples.

2.2 Materials and Methods

Study Design

The experimental protocol was approved by the Louisiana State University Institutional Animal Care and Use Committee (IACUC) (Protocol #14-069). Ten clinically healthy Thoroughbred horses (two - five years of age and weighing between 409 kg and 570 kg) were obtained via donation to the Louisiana State University Equine Health Studies Program. Medical history of the horses was unknown at the time of donation; however, prior to enrollment in the current study, all horses underwent at least a two-week isolation and washout period following donation. Horses were randomly assigned using a coin flip to either a treatment (n=5) or control group (n=5). The surgeon, who was not involved in subsequent analyses, was not masked to treatment groups. All personnel who took part in the data collection and analysis were masked to treatment groups.

Bone biopsies were taken from each horse at Day 0 (baseline before treatment) and Day 60 (60 days post-treatment) (Figure 2.1). This time frame was determined by previous studies that showed a positive effect of tiludronate administration in horses 60 days post initiation of treatment (Denoix et al., 2003, Coudry et al., 2007, Gough et al., 2010). The right or left tuber coxarum was randomly selected, via coin flip, for the first biopsy (outlined below in “Surgical Procedure”). Immediately following the initial biopsy surgery (Day 0), each horse was administered tiludronate (1 mg/kg, diluted in 1L of 0.9% saline, IV) or equal volumes of saline. The tiludronate solution was administered over 90 minutes using an IV fluid pump. The horses stood in the stocks during this infusion and were monitored for signs of colic. Sixty days later, the contralateral tuber

coxarum was biopsied in the same manner. Prior to the second biopsy, oxytetracycline (Vetrimycin 100, VetOne, Boise, ID, USA) was administered at Day 47 and Day 57 as a fluorochrome label to identify bone remodeling parameters. Biopsies were evaluated with microCT and histomorphometry for changes in bone morphology and remodeling rates, as outlined below under “MicroCT” and “Histology.”

Tiludronate



Figure 2.1 Tiludronate study design schematic of time line, outlining biopsy collection and treatment administration. Abbreviations: Contra., Contralateral; Ipsi., Ipsilateral.

Study Horses

Thoroughbred horses, as outlined above under “Study Design”, were included if they were free from outward musculoskeletal disease and clinically healthy, as assessed by a boarded veterinary surgeon (CFM) during a physical exam, and included seven geldings and three fillies with a mean age of 3.5 years (control age: (mean \pm SD) 3.4 ± 1.14 years; weight: 500.6 ± 44.8 kg; treated age: 3.6 ± 1.34 years). Sample sizes were influenced based on donation availability, and all eligible horses were considered. Additionally, if eligible horses became available during the course of data collection, they were evaluated and included in order to maximize sample size. Throughout the study, they were housed in individual stalls following the biopsies and then turned out in

groups in pastures. They were fed free choice hay and water, with grain being provided twice daily.

In addition to the aforementioned horses, biopsies were also obtained from three additional horses euthanized for non-musculoskeletal related reasons at the Louisiana Disease and Diagnostic Laboratory (LADDL). These were samples of convenience, obtained at necropsy from horses not included in this study. These horses were aged 9 months, 1 year, and 25 years, and were used to compare histopathological changes within the biopsies with age. The samples were obtained using the same surgical technique, as described below, but were not enrolled in the pharmacologic evaluations.

Surgical Procedure & Treatment

Horses were sedated with intravenous (IV) xylazine (Xylamed, Bimeda, Cambridge, ON Canada) (0.35 to 0.5 mg/kg). The surgical method has been previously published in detail (Mitchell et al., 2017). In short, the biopsy site was centered on the proximal palpable protuberance of the tuber coxarum. A rectangular region (approximately 10 cm X 10 cm) was clipped around the tuber coxarum and then aseptically prepared. Lidocaine (Lidocaine 2%, VetOne, Boise, ID, USA) was injected subcutaneously, deep to the proposed incision site in a vertical line, centered on the palpable tuber coxarum, extending 4 cm proximal and distal to that palpable point and then deeply, adjacent to the periosteum of the tuber coxarum. The horse was further sedated with detomidine hydrochloride (Dormosedan, Zoetis, Kalamazoo, MI, USA) (3 to 5 mg IV) and butorphanol tartrate (Torbugesic, Fort Dodge, New York, NY, USA) (3 to 5 mg IV) prior to making the skin incision (Mitchell et al., 2017).

A 6-8 cm, vertically oriented incision was made over the tuber coxarum (Figure 2.2A), and dissected to expose the cranial, caudal, proximal and deep margins. The periosteum was incised with a #15 blade in a cranial to caudal direction on the lateral edge of the tuber coxarum, at least 1 cm distal to the proximal portion of the protuberance. An oscillating saw was used to transect the protuberance of the tuber coxarum, with the saw blade angled either parallel to the ground or slightly dorsally, depending upon the position of the limb and the horse's pelvic anatomy. In order to limit thermal damage, the saw blade was continuously lavaged with saline. Depending upon the direction of the saw cut, the bone biopsy (Figure 2.2B) was either removed, or detached from soft tissue prior to removal. The excised section of bone representing the biopsy was at least 1 cm tall, with the width and length of the biopsy dependent on each horse's pelvic anatomy. The goal was to obtain the largest biopsy possible without cutting into the iliac crest on the deep border of the tuber coxarum. If necessary, the horizontal cut was moved distally and the saw blade angled in a more proximal direction to produce a biopsy of suitable size. The surgery site was lavaged, and the subcutaneous tissue was sutured with 2-0 polyglactin 910 in a simple continuous pattern. The skin was sutured using 0 polypropylene in either a Ford interlocking or cruciate pattern. An aluminium based bandage spray (Aluspray, Neogen Corporation, Lexington, KY, USA) was applied to the surgery site and a lidocaine patch (Lidocaine Patch 5%, Qualitest, Huntsville, AL, USA) was then applied over the incision (Mitchell et al., 2017).

Following the initial biopsy (Day 0 to 1), horses were stalled for at least 24 hours and monitored every 2 hours over the first 24-hour period using a visual pain score

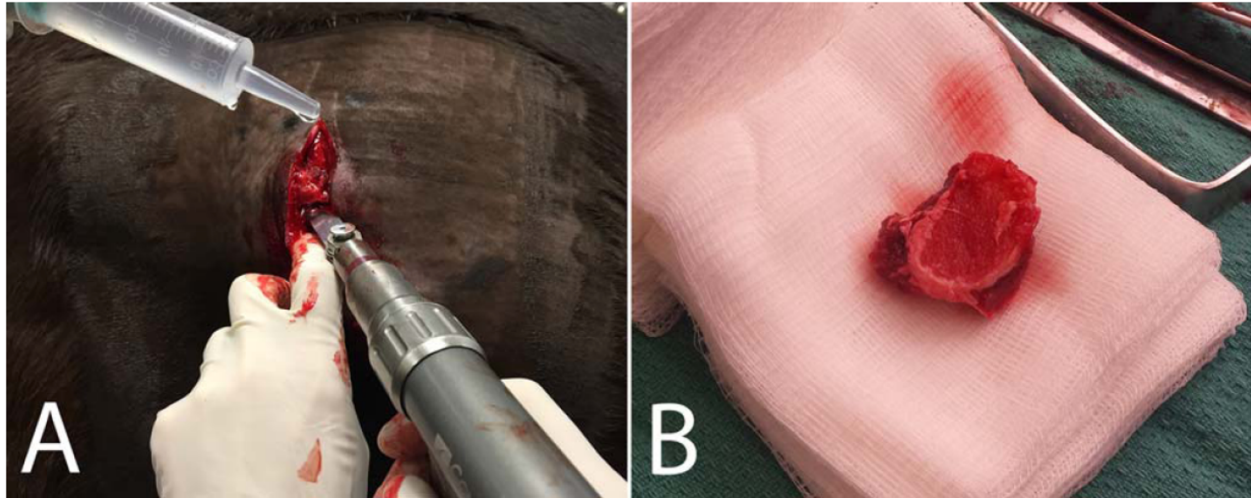


Figure 2.2 Bone biopsy from the tuber coxarum in a horse. A) The incision is centered over the palpable dorsal protuberance of the tuber coxarum. The excised piece of tuber coxarum is directly above the saw blade, with a small amount of connective tissue on its superficial edge. Cranial to the left of image, proximal to the top of image. B) Bone biopsy harvested. Cut surface facing up, resting on a 10.1 X 10.1 cm gauze square. MicroCT

(Doherty and Valverde, 2006). After 24 hours, horses were returned to their respective pastures and checked daily for signs of lameness or incisional complications until suture removal at 14 days post biopsy. At Day 47 and 57 post biopsy, the horses were treated with 25 mg/kg of oxytetracycline administered slowly IV. Sixty days after the initial biopsy, the contralateral tuber coxarum was biopsied using the same surgical methods as described above. However, after surgery, horses were administered flunixin meglumine (Prevail, Bimeda, Cambridge, ON, Canada) (1.1 mg/kg IV) as an additional analgesic. Surgical aftercare was identical to above from post-surgery to 14 days later when the sutures were removed.

MicroCT

Following biopsy, tuber coxae samples were dissected free from tissue and fixed in 10% non-buffered formalin for seven days, then transferred to and stored in 70% ethanol at 20°C. Samples were placed in holders with 70% ethanol for scanning by microCT (Scanco model 40, Scanco Medical AG, Basserdorf, Switzerland). Biopsies were scanned at 55kV, 0.3-second integration time, with a 30 µm voxel size in plane and a 30 µm slice thickness. The region of interest was determined for trabecular bone. The proper threshold for image segmentation was tested, with the same threshold being used throughout the experiment. Trabecular bone was evaluated for bone volume (BV), total volume (TV), BV/TV, tissue mineral density, trabecular number (Tb.N), trabecular thickness (Tb.Th), trabecular spacing (Tb.Sp), connectivity density (Conn.D) and structural model index (SMI) based on established procedures and nomenclature (Bouxsein et al., 2010).

Histology

Following microCT evaluation, biopsies were prepared for histology. Day 0 biopsies were prepared for decalcified histology, and Day 60 biopsies were prepared for undecalcified histology so visualization of fluorochrome labels was possible. Due to differences in preparation techniques between decalcified and undecalcified histology, and size of slides used for each, histological preparation of both sets of biopsies differed slightly. However, care was taken to ensure sections from each biopsy were taken in the same location and plane of section, regardless of preparation method. Day 0 biopsies were decalcified with 10% ethylenediaminetetraacetic acid (EDTA) and

prepared for routine paraffin embedding. In order to fit on glass histological slides, Day 0 biopsies were split in half and embedded separately. This resulted in 6 – 8, 4 μm thick sections per biopsy that were stained with hematoxylin and eosin (H&E). Day 60 biopsies were prepared intact for undecalcified histology and two, 45-60 μm thick sections were produced. The first was stained with Stevenel's Blue and Van Gieson's picro fusion for evaluation by static histomorphometry, and the second section was left unstained for evaluation by dynamic histomorphometry. Although histological slides for Day 0 and Day 60 biopsies were prepared differently for ease of handling, all bony features were easily discernable and comparable in both sets of slides, as outlined in Figure 2.3 (Dempster et al., 2013).

All biopsy sections were evaluated for quality under light microscopy as previously described (Steiger et al., 1999). In short, cortical and trabecular bone in each section were evaluated using a semi-quantitative scale whereas tissue was determined to be useless (0), poor (1), or good (2) quality. Three individuals (including one boarded veterinary pathologist, one established orthopedic researcher and one graduate student), evaluated each slide. Some biopsies had multiple sections to evaluate and all sections generated a score that was then averaged for each biopsy.

All bone histomorphometry evaluations were performed using histomorphometry software (Osteomeasure© Bone Histomorphometry System, Osteometrics, Inc., Decatur, GA, USA) following standard procedures and nomenclature (Dempster et al., 2013). Static histomorphometry parameters included direct measurements of: BV, marrow volume (Ma.V), bone surface (Crook et al.), eroded surface (ES), mineralized surface (Md.S), osteoblast surface (Ob.S), osteoblast number (Ob.N), osteoclast

number (Oc.N), osteoclast surface (Oc.S) and remodeling surface (RS). Indirect measurements included: Tb.N, Tb.Th, Tb.Sp and the aforementioned direct measurements standardized to respective areas and volumes. Dynamic histomorphometry included mineralizing surface per bone surface (MS/BS), mineral apposition rate (MAR) and the bone formation rate per bone surface (BFR/BS).

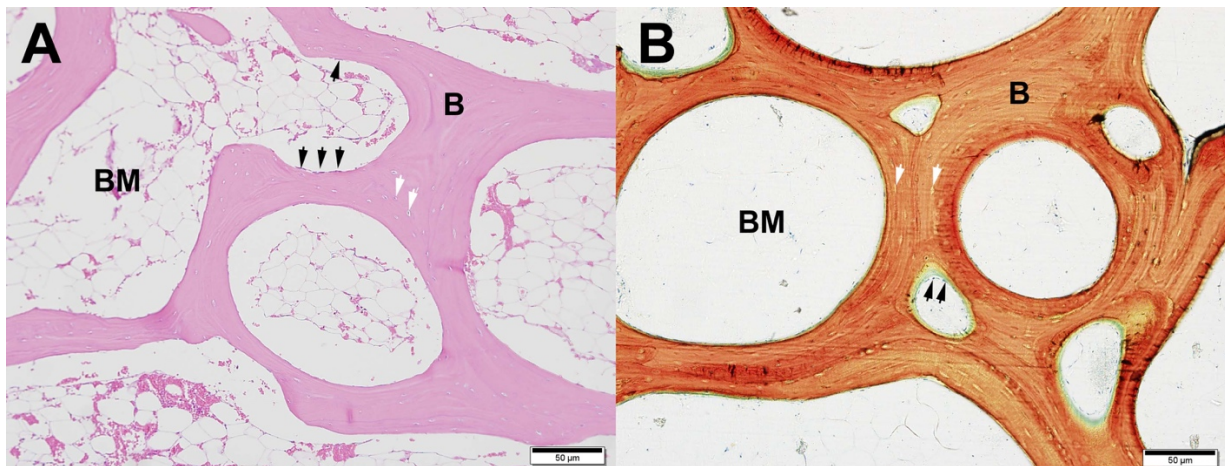


Figure 2.3 Labeled histological sections of bone biopsies. Representative A) decalcified and B) un-decalcified histological sections of biopsy 2 (Day 60), highlighting similar trabecular bone features. Abbreviations: B, bone; BM, bone marrow. Black arrows = osteoblasts; white arrows = osteocytes.

Statistics

To evaluate slide quality, trabecular bone quality scores were averaged and the standard deviation was calculated. To evaluate the effect of tiludronate on bone, microCT and histomorphometry data were analyzed using independent analyses between treatment groups, as well as dependent analyses between biopsies. Data were tested for normality using the Shapiro-Wilk test and depending on normality, either parametric or non-parametric analyses were used (i.e., Student's t-test or related samples Wilcoxon signed rank test, respectively). A related-sample test was used to

evaluate changes from biopsy 1 (Day 0) to biopsy 2 (Day 60) within the control or treated horses. An unrelated-sample test was performed to evaluate difference between treated and control horses within biopsy 2. Statistical analyses were performed using commercially-available software (SPSS, version 22, IBM Corporation, Armonk, NY, USA), and p-values of <0.05 were considered significant.

2.3 Results

Surgical Technique

Horses received between 408 – 500 mg (mean \pm SD, 474.6 \pm 38.6 mg) of tiludronate based on weight. Only one of the ten horses in the study experienced incisional dehiscence, but this complication resolved with minimal medical intervention. All of the other 19 biopsies healed uneventfully, with no horses displaying any rear limb lameness or ratable discomfort at any time over the duration of this study. All biopsies obtained were adequate for all analyses (mean volume of 3123.72 mm³ \pm 1495.37 mm³ (SD) as measured via microCT) (Mitchell et al., 2017).

MicroCT

The biopsies were consistent in size and shape between both biopsies and treatment groups (Figure 2.4). No significant differences in TV were identified between treatment groups or biopsy as evaluated by microCT (Figure 2.5). Overall, tiludronate did not significantly alter bone morphology parameters after 60 days when compared to saline. In addition, there were no significant differences in morphology parameters between biopsies within treated horses or control horses (Figure 2.5).

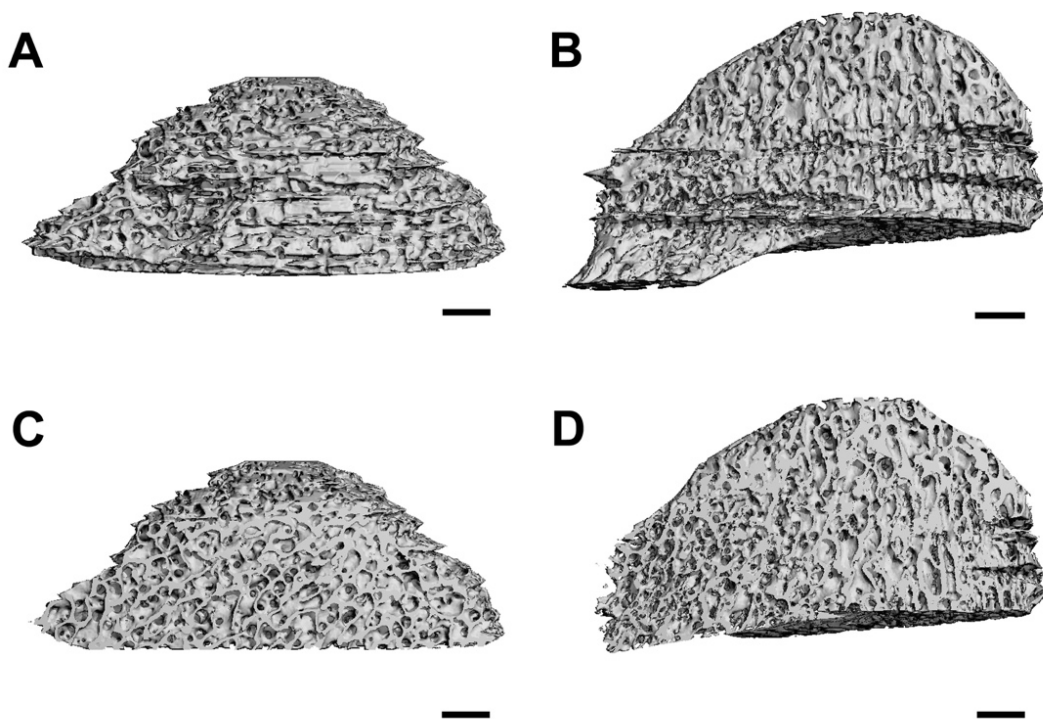


Figure 2.4 Representative Day 0 bone biopsies for control (A,C) and treated (B,D) horses, showing the entire biopsy, excluding cortical bone (A,B), and a visually-sectioned view (C,D), highlighting the trabecular bone architecture. The ventral face is the surgically-cut surface. Bar = 2 mm.

Histopathology and Slide Quality

Microscopic examination showed all sections consisted of irregularly triangular, dome-shaped, or rectangular sections of mature bone containing variable amounts of compact cortical bone and attached ligaments, tendon and associated skeletal muscle, lamellar trabecular bone and marrow spaces. The quality of the trabecular bone within all biopsies was good (Figure 2.6), with adequate bony tissue for evaluation trabecular bone.

		Saline		Tiludronate	
		Day 0	Day 60	Day 0	Day 60
MicroCT	BV/TV (%)	0.3 ± 0.06	0.3 ± 0.09	0.3 ± 0.04	0.3 ± 0.05
	TbTh (mm)	0.1 ± 0.02	0.2 ± 0.03	0.1 ± 0.01	0.2 ± 0.02
	TbN (/mm)	1.7 ± 0.27	1.6 ± 0.23	1.7 ± 0.17	1.8 ± 0.24
	BS/BV (%)	15.0 ± 2.73	13.4 ± 2.63	14.5 ± 1.08	13.9 ± 1.50
Static Histomorphometry	BV/TV (%)	28.9 ± 13.91	27.6 ± 13.10	24.1 ± 7.19	30.8 ± 6.82
	Ob.N/TA (/mm²)	46.4 ± 15.18	66.3 ± 32.40	17.6 ± 9.86	11.3 ± 6.15
	Oc.N/TA (/mm²)	0.6 ± 0.46 ^a	0.01 ± 0.02 ^a	0.6 ± 0.41	0.1 ± 0.11
Dynamic Histomorphometry	sL.S/BS (%)		29.0 ± 4.47		24.4 ± 7.00
	dL.S/BS (%)		4.7 ± 1.88		6.3 ± 4.59
	MAR (µm/d)		1.2 ± 0.20		1.2 ± 0.21

Figure 2.5 Summary data (mean ± SD) of bone structure and remodeling parameters from biopsy 1 (Day 0) and biopsy 2 (Day 60) for microCT analyses, static histomorphometry analysis and dynamic histomorphometry analysis in control (n=5) and treated (n=5) horses. Abbreviations: BV/TV, bone volume fraction (bone volume/total volume); Tb.Th, trabecular thickness; Tb.N trabecular number; BS/BV, bone surface/bone volume; Ob.N/TA, number of osteoblasts per tissue area; Oc.N/TA, number of osteoclasts per tissue area; sL.S/BS, single label surface per bone surface; dL.S/BS, double label surface per bone surface; MAR, mineral apposition rate. ^aSignificant (P ≤ 0.05) difference between values with the same letter superscript. P-value results from related samples Wilcoxon Signed Rank Test.

Horse	Biopsy	Trabecular Bone
1	1	1.67 (± 0.52)
	2	2 (± 0)
2	1	1.83 (± 0.39)
	2	2 (± 0)
3	1	2 (± 0)
	2	2 (± 0)
4	1	2 (± 0)
	2	2 (± 0)
5	1	1.75 (± 0.45)
	2	2 (± 0)
6	1	2 (± 0)
	2	2 (± 0)
7	1	2 (± 0)
	2	1.67 (± 0.58)
8	1	1.75 (± 0.40)
	2	2 (± 0)
9	1	1.83 (± 0.39)
	2	1.67 (± 0.58)
10	1	1.83 (± 0.39)
	2	2 (± 0)

Figure 2.6 Mean (\pm SD) histological bone biopsy scores from each horse enrolled in the study. The quality scores were categorized as follows: useless (0), poor quality (1), good quality (2).

Sections contained variable amounts of artifact from collection, including presence of bone dust, mild hemorrhage, coagulative necrosis of skeletal muscle or bone and rare trabecular fractures. In most sections, these artifacts were present at the margins of the sections examined, only rarely extending into more central aspects of the sections, and therefore did not affect interpretations of the majority of the tissue sample.

Any area of compromised architecture or artifact did not extend any more than 2 mm away from the cut surface in any of the biopsies.

Most horses (8/10) and most sections (12/18) showed variable sized foci of mature hyaline cartilage present scattered throughout the endocortical spaces. These were rare (one - three small islands) in some sections, but numerous in others. Foci ranged from irregularly round or oval, to polygonal to linear, and were frequently surrounded by variable amounts of mature, lamellar trabecular bone. Occasionally, within the round to oval foci, the hyaline cartilage surrounded an open central region containing blood vessels within adipose and loose fibrous connective tissues (Figure 2.7A). In some cartilage islands, there were variably sized regions of necrosis or areas of mineralization. Occasionally, the chondrocytes within the viable areas of cartilage formed distinct rows and demonstrated ordered chondrocyte maturation, similar to that seen in physal growth plates (Figure 2.7B). These features were especially prominent in more linear foci of hyaline cartilage. In some sections, there were more subtle foci of mineralized cartilage completely surrounding by and embedded in mature, lamellar, trabecular bone (Figure 2.7C). There were variable amounts of mature hyaline or fibrocartilage blending with the adjacent ligament at the margins of most sections along the periosteal surface of the cortical bone, consistent with ligament attachment sites. Occasionally, irregularly linear tongues of cartilage extended from these regions into the adjacent marrow spaces (Figure 2.7D). In addition to the apophyses, these sections contained individual foci of hyaline cartilage within the endocortical spaces. Some of these foci were closely associated with the growth plate and/or hyaline cartilage within areas of ligament attachments.

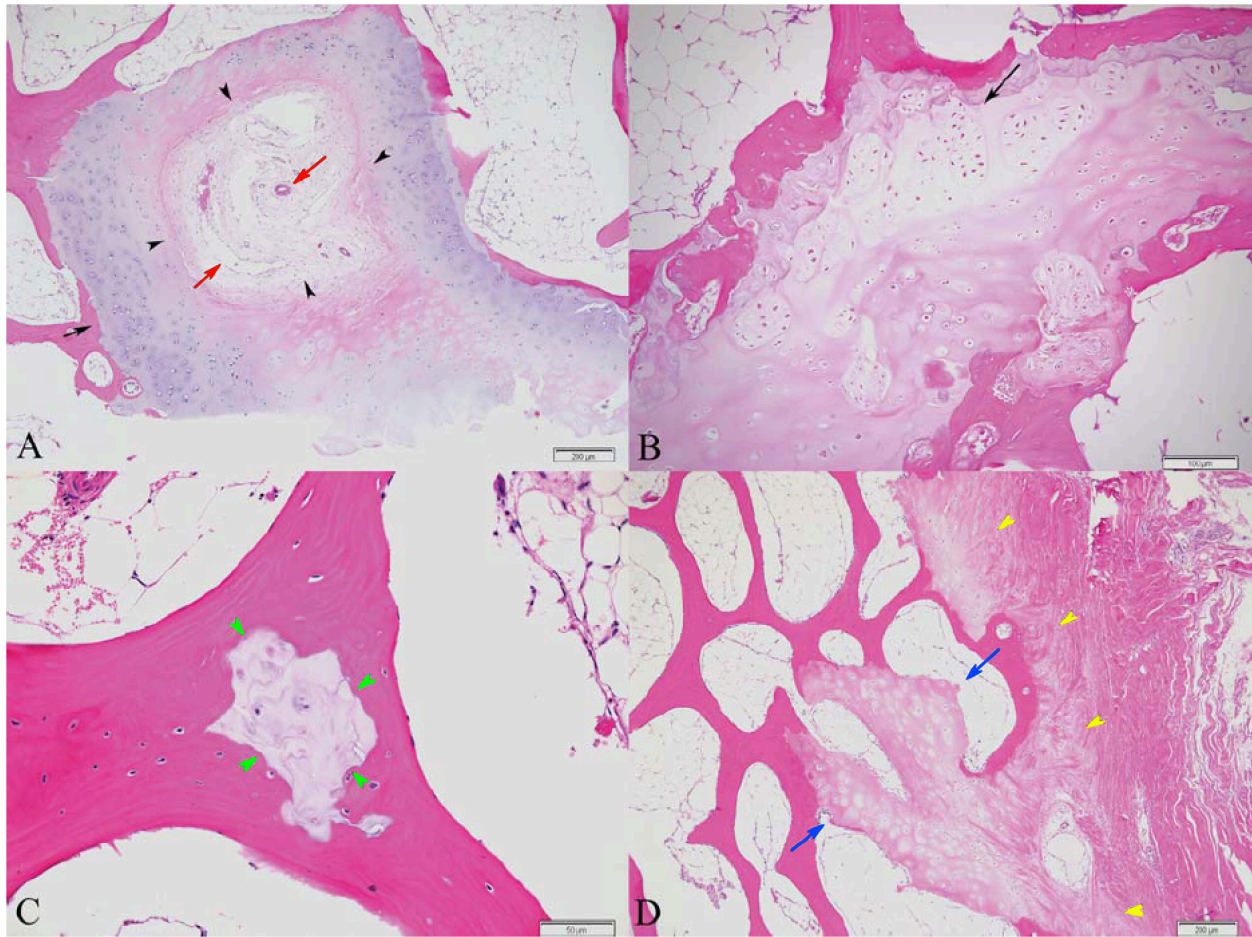


Figure 2.7 Histologic images of cartilage foci within endocortical spaces. A) Hyaline cartilage with central region composed of loose fibrous connective and adipose tissues (bounded by arrowheads) containing numerous blood vessels (red arrows). B) Cartilage with chondrocyte maturation (black arrows). C) Mineralized cartilage foci (bounded by green arrowheads) embedded within mature trabecular bone. D) Cartilage tongues (blue arrows) extending from a site of ligament attachment (yellow arrowheads) into endocortical space.

Additional samples from 3 horses of a range of ages (i.e., 9 months, 1 year, 25 years) not included in the experiments were examined for comparison to the study horses. The sections from the 9-month and 1-year-old horses were histologically similar and contained linear, mature growth plate cartilage within the endocortical space, consistent with an apophyseal growth plate. These apophyses exhibited normal

chondrocyte maturation including distinguishable resting, proliferative, hypertrophic, and mineralization zones (Figure 2.8).

In addition to the apophyses, these sections contained individual foci of hyaline cartilage within the endocortical spaces, similar to those present in the previously described study samples. Some of these foci were closely associated with the growth plate and/or hyaline cartilage within areas of ligament attachments. In one section of the 1-year-old horse, there was an area within the peripheral cortical hyaline cartilage that demonstrated orderly chondrocyte maturation similar to that within the apophysis (Figure 2.8B). In contrast to the study animals, the marrow spaces in these two animals was often highly cellular.

In the 25-year-old horse, there was a single small focus of mineralized cartilage embedded within trabecular bone. There were no other regions of hyaline cartilage within the endocortical space. At the ligament attachment sites associated with the cortical bone, there was less cartilage present than in the previously described slides.

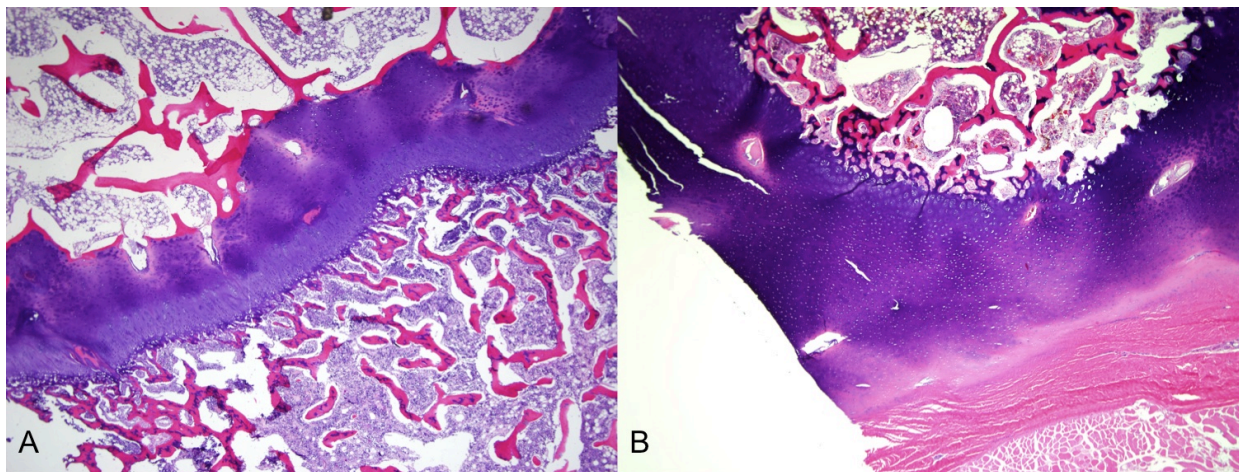


Figure 2.8. Histologic images from juvenile horse demonstrating active bone formation. (A) Histologic image containing an apophyseal growth plate with distinct resting, proliferation, hypertrophic, and mineralization zones; (B) Histologic image demonstrating a region of bone formation associated with the hyaline cartilage at a ligament attachment site.

The cartilage present consisted of fibrocartilage, rather than hyaline cartilage. The marrow spaces contained adipose tissue and no cellular bone marrow.

Histology

As evaluated using static histomorphometry, no significant differences were identified between treatment groups. When comparing biopsies within each treatment group, tiludronate significantly decreased trabecular thickness ($p=0.02$) and increased BS/BV ratio ($p=0.048$) when comparing Day 60 biopsies to Day 0 biopsies. Some measurements were significantly different when comparing the Day 60 biopsy to the Day 0 biopsy for the saline group: a decrease in RS/BS ($p=0.04$), decrease in BS/TV ($p=0.04$), decrease in Oc.N/TA ($p=0.04$) (Figure 2.5) and a decrease in Oc.S/BS ($p=0.04$).

As evaluated using dynamic histomorphometry, after 60 days, tiludronate did not significantly alter bone remodeling parameters when compared to saline. Overall, bone apposition rates and bone turnover was very similar between treated and control groups (Figure 2.5).

2.4 Discussion

This report describes the effect of a single administration of tiludronate on bony cells, trabecular bone morphology and bone remodeling in ten clinically healthy, young horses. A previous study utilizing a bone biopsy model attempted to elucidate changes in bone morphology secondary to tiludronate treatment in horses, but, the samples

obtained were inadequate for evaluation of bone morphology and remodeling (Delguste et al., 2011). Thus, to our knowledge, this is the first reported study evaluating the cellular and structural effect on bone secondary to tiludronate administered in horses. There were no significant effects of tiludronate (1 mg/kg, IV) on bony cells or bone structure and remodeling parameters 60 days after a single administration in young horses. Although a few parameters were significantly different for the control group, we believe that these are changes that could occur during normal bone turnover in young horses, and these select changes do not make substantial biological sense when all variables are considered. It is possible, however, that these are select bony changes that occur during normal bone turnover in young horses, and tiludronate prevented similar changes from occurring. No differences were noted between treatment groups within the same biopsy. Although there was a significant increase in trabecular thickness between biopsies in horses treated with tiludronate, as determined by static histomorphometry, this change was not corroborated with microCT evaluations, which provides a more comprehensive evaluation of bone morphology within the biopsies.

It is possible that the time frame (60 days) evaluated in this study was not long enough to evaluate overall changes in bone remodeling. However, this time frame was selected based on the only published data regarding the effect of tiludronate on horses, which found a positive effect of tiludronate after 60 days (Denoix et al., 2003, Coudry et al., 2007, Gough et al., 2010). In addition, a study evaluating bone remodeling in horses following treatment with phenylbutazone, which, unlike tiludronate, is not utilized as a treatment for diseases of bone remodeling, found significant changes in MAR using similar sample sizes after only 30 days (Rhode et al., 2000). Therefore, if tiludronate

was to have an impact on bone remodeling in young horses at the dose given, it would be expected that normal bone apposition rates in horses should be at least minimally affected by tiludronate within the timeframe of the present study. However, it is possible that diseased bone, characterized by abnormal bone remodeling, could be impacted by tiludronate administration more than the results shown in this study on normal bone. A study that identified significant improvements in lameness secondary to distal tarsal joint osteoarthritis 60 days post treatment with tiludronate also identified significant reductions in periarticular osteophyte formation at that time point, as evaluated by radiographs, indicating a potential influence on bone remodeling in horses (Gough et al., 2010). Therefore, these data also support the chosen time point at which to identify potential changes in bone microarchitecture. However, future studies including additional time points post treatment would be required to confirm whether tiludronate has a significant impact on bone morphology. As such, more recent data evaluating effectiveness of tiludronate administration on lameness associated with navicular disease as evaluated by more objective force platform analyses found significant improvements 120 and 200 days post treatment, but not after 60 days (Whitfield et al., 2016).

Due to the nature of a pilot study, there was a low sample size of 5 horses per group. Therefore, the effect of tiludronate on bone remodeling and structure may not have been apparent in the data presented here. Overall, it is possible that tiludronate has a small effect that was not identified in the present study. However, a difference to some degree was expected, despite the low numbers, given the power of tiludronate as a modifier of bone remodeling in numerous other species (Rhode et al., 2000). The fact

that there was no difference between treatment groups or biopsies within the same horse warrants further investigation into the efficacy of tiludronate as a treatment for diseases of bone remodeling in the horse at the current dosage recommended.

Tiludronate therapy is widely used in the veterinary clinical setting to treat disorders involving abnormal bone remodeling, including distal tarsal joint osteoarthritis (Gough et al., 2010), thoracic & lumbar vertebral arthritis (Coudry et al., 2007) and dorsal metacarpal disease (Carpenter, 2012). The efficacy of tiludronate has been shown in young animals in other species, including a reduction of trabecular bone resorption adjacent to growth plates and increased bone density in skeletally immature rats and baboons (Geusens et al., 1992). Tiludronate has been previously evaluated for pathological bone changes in horses aged 4 years and older (FOI, 2014); however, despite the manufacturer's recommendation to avoid administration of tiludronate to horses less than four years of age, clinicians are administering this drug to horses that are younger than four years of age as a treatment for dorsal metacarpal disease (Carpenter, 2012). It is well known that younger horses undergo more rapid bone remodeling than skeletally mature adults (Goyal et al., 1981), so this study aimed to also evaluate the effect of tiludronate administration in young horses, where negative impacts on normal bone remodeling could result in significant clinical outcomes in young equine athletes. While the current study population included horses four and five years of age, biopsies from all horses within the study included evidence of an open apophysis for the tuber coxae (Mitchell et al., 2017), indicating some degree of skeletal immaturity. Additionally, the same biopsy taken from a 25-year-old mare, which can be reasonably assumed to be skeletally mature, showed no presence of an

apophysis or retained hyaline cartilage foci. Thus, it appears that there is likely complete closure of the apophyseal growth plate and transition of the superficial hyaline cartilage to mature fibrocartilage associated with skeletal maturity, which was not present in the evaluated horses. Additionally, although subjective and not quantitatively evaluated, one evaluator noticed an increase in the size and number of cartilage foci in samples in the younger horses. However, due to the large age gap between the horses included in the study and the 25-year-old evaluated, it is unclear when the apophyses in the tuber coxarum disappear. Horses in the current study were also not strictly age-matched; however, the means and standard deviations for each group were almost identical. In addition, dependent analyses comparing biopsies within each horse were performed, thereby serving as a more robust analysis of changes secondary to treatment. As outlined above, we did not see any influence on bone remodeling or morphology in this young population. However, due to the small sample sizes for each age included in the study and the known effect of age on bone remodeling parameters, there cannot be definitive conclusions based on age. In addition to a larger number of horses, a smaller range of ages in horses may result in a significant effect on bone morphology parameters.

The iliac biopsy location utilized in the study was chosen for multiple reasons, despite the dissimilarities in architecture and biomechanics to weight bearing bones found in the equine distal limb, such as the metacarpal bones. Most importantly, the tuber coxarum is an easily accessible location that allowed for a non-terminal biopsy model in the equine, and provides the opportunity for multiple biopsies from the same horse over set time points (Mitchell et al., 2017). Various sites for bone biopsy have

been described in standing sedated, anesthetized and euthanized horses (Delguste et al., 2011). These locations include the sternbrae, ribs, tuber coxae, the third metacarpal bone, and the fourth tarsal bone (Misheff et al., 1992, Steiger et al., 1999, Désévaux et al., 2000, Delguste et al., 2011). Biopsies obtained in these studies have ideally been as small as possible due to the relative size of the bone being sampled (ribs) or due to the load-bearing nature of the bone (metacarpus) (Firth, 2004). Biopsies obtained from weight bearing bones, such as the metacarpals and tarsal bones, deemed of adequate size for histologic examination would likely result in lameness or euthanasia of the horse. In addition, these samples would provide little, if any, trabecular bone for examination, as these bones are composed of predominantly cortical bone. Larger biopsies from non-weight-bearing bones provides more data for consistent histological and architectural examination, as shown in this study.

Despite the differences in biomechanics, bone remodeling of the tuber coxarum has been shown to accurately predict the effect of alendronate, another form of bisphosphonate, on non-homogenous skeletal locations in the body (i.e., vertebral column) (Mashiba et al., 2005). This location was chosen for the biopsy site for the additional reason that it has been shown that bisphosphonates accumulate at the highest density in tuber coxae when compared to other bones in the equine, including bones that experience more biomechanical stress, such as the 3rd metacarpal, rib and cuboid bone (Delguste et al., 2011). An added benefit of this biopsy technique was the relatively large biopsy size, which allowed multiple study endpoints to be utilized. The second biopsy was prepared for undecalcified histology in order to preserve the fluorescent label, which required different preparation than the initial biopsy received.

Although preparation methods varied, methods of analyses and outcome measures were identical for both preparation methods of static histomorphometry sections (Dempster et al., 2013).

It is important to recognize that this technique for biopsy has potential to include the apophyseal growth plate or remnants thereof, particularly in younger horses. The specific apophyses in the bones of the pelvis in the horse are not well described and the presence of an apophysis in the tuber coxarum has not been substantiated in the literature of domestic quadrupeds. The identification of an apophysis in the tuber coxarum is an important finding and the presence of cartilaginous foci should be noted for future studies using this biopsy method as it may bias assessment of trabecular bone that rely on counts of trabecular number and spacing. However, the presence of these foci do provide a potentially unique opportunity for investigators examining changes in bone growth and physeal activity in horses.

In conclusion, this study describes a simple tuber coxarum biopsy procedure for horses that is well tolerated and produces samples large enough to be sectioned multiple times, permitting several methods of analyses to evaluate bone morphology and remodeling in a non-terminal model. It appears that tiludronate does not have a substantial impact on normal bone remodeling kinetics and morphology in young horses 60 days post treatment. Overall, tiludronate does not appear to impact bone remodeling parameters in young horses, and has minimal to no effect on bone morphology parameters after 60 days.

2.5 References

- Bouxsein, M. L., S. K. Boyd, B. A. Christiansen, R. E. Guldberg, K. J. Jepsen and R. Müller (2010). "Guidelines for assessment of bone microstructure in rodents using micro-computed tomography." J Bone Min Res **25**(7): 1468-1486.
- Carpenter, R. (2012). How to treat dorsal metacarpal disease with regional tiludronate and extracorporeal shock wave therapies in Thoroughbred racehorses. AAEP Annual Convention.
- Coudry, V., D. Thibaud, B. Riccio, F. Audigié, D. Didierlaurent and J.-M. Denoix (2007). "Efficacy of tiludronate in the treatment of horses with signs of pain associated with osteoarthritic lesions of the thoracolumbar vertebral column." Am J Vet Res **68**(3): 329-337.
- Crook, T. C., S. E. Cruickshank, C. M. McGowan, N. Stubbs, A. M. Wilson, E. Hodson-Tole and R. C. Payne (2010). "A comparison of the moment arms of pelvic limb muscles in horses bred for acceleration (Quarter Horse) and endurance (Arab)." J Anat **217**(1): 26-37.
- David, P. E., H. Nguyen, A. Barbier and R. Baron (1996). "The bisphosphonate tiludronate is a potent inhibitor of the osteoclast vacuolar H⁺-ATPase." J Bone Miner Res **11**(10): 1498-1507.
- Delguste, C., H. Amory, M. Doucet, C. Piccot-Crézollet, D. Thibaud, P. Garnero, J. Detilleux and O. M. Lepage (2007). "Pharmacological effects of tiludronate in horses after long-term immobilization." Bone **41**(3): 414-421.
- Delguste, C., M. Doucet, A. Gabriel, J. Guyonnet, O. M. Lepage and H. Amory (2011). "Assessment of a bone biopsy technique for measuring tiludronate in horses: a preliminary study." Can J Vet Res **75**(2): 128-133.
- Dempster, D. W., J. E. Compston, M. K. Drezner, F. H. Glorieux, J. A. Kanis, H. Malluche, P. J. Meunier, S. M. Ott, R. R. Recker and A. M. Parfitt (2013). "Standardized nomenclature, symbols, and units for bone histomorphometry: a 2012 update of the report of the ASBMR Histomorphometry Nomenclature committee." J Bone Miner Res **28**(1): 1-16.
- Denoix, J. M., D. Thibaud and B. Riccio (2003). "Tiludronate as a new therapeutic agent in the treatment of navicular disease: a double-blind placebo-controlled clinical trial." Equine Vet J **34**(4): 407-413.
- Désévaux, C., S. Laverty and B. Doizé (2000). "Sternal bone biopsy in standing horses." Vet Surg **29**: 303-308.
- Doherty, T. and A. Valverde (2006). Manual of equine anaesthesia and analgesia, Blackwell Publishing.

- Firth, E. C. (2004). "Problems in quantifying bone response to exercise in horses: a review." N Z Vet J **52**(5): 216-229.
- FOI. (2014). "Freedom of Information Summary: For the control of clinical signs associated with navicular syndrome in horses." from <https://www.fda.gov/downloads/AnimalVeterinary/Products/ApprovedAnimalDrugProducts/FOIADrugSummaries/UCM396896.pdf>.
- Geusens, P., J. Nijs, G. Van der Perre, R. Van Audekercke, G. Lowet, S. Goovaerts, A. Barbier, F. Lacheretz, B. Remandet and Y. Jiang (1992). "Longitudinal effect of tiludronate on bone mineral density, resonant frequency, and strength in monkeys." J Bone Miner Res **7**(6): 599-609.
- Gough, M. R., D. Thibaud and R. K. W. Smith (2010). "Tiludronate infusion in the treatment of bone spavin: a double blind placebo-controlled trial." Equine Vet J **42**(5): 381-387.
- Goyal, H., F. MacCallum, M. Brown and J. Delack (1981). "Growth rates at the extremities of limb bones in young horses." Can Vet J **22**(2): 31.
- Henneman, Z. J., G. H. Nancollas, H. F. Ebetino, G. R. G. Russell and R. J. Phipps (2008). "Bisphosphonate binding affinity as assessed by inhibition of carbonated apatite dissolution in vitro." J Biomed Mater Res A **85A**(4): 993-1000.
- Kamm, L., W. McIlwraith and C. Kawcak (2008). "A review of the efficacy of tiludronate in the horse." J Equine Vet Sci **28**(4): 209-214.
- MacNeil, J. A. and S. K. Boyd (2007). "Accuracy of high-resolution peripheral quantitative computed tomography for measurement of bone quality." Med Eng Phys **29**: 1096-1105.
- Mashiba, T., S. Hui, C. H. Turner, S. Mori, C. C. Johnston and D. B. Burr (2005). "Bone Remodeling at the Iliac Crest Can Predict the Changes in Remodeling Dynamics, Microdamage Accumulation, and Mechanical Properties in the Lumbar Vertebrae of Dogs." Calcif Tissue Int **77**(3): 180-185.
- Misheff, M. M., S. M. Stover and R. R. Pool (1992). "Corticocancellous bone biopsy from the 12th rib of standing horses." Vet Surg **21**(2): 133-138.
- Mitchell, C. F., H. A. Richbourg, B. A. Goupil, A. N. Gillett and M. A. McNulty (2017). "Assessment of tuber coxae bone biopsy in the standing horse." Vet Surg.
- Müller, R., V. H. Campenhout, V. B. Damme, G. V. D. Perre, J. Dequeker, T. Hildebrand and P. Rueggesser (1998). "Morphometric analysis of human bone biopsies: a quantitative structural comparison of histological sections and micro-computed tomography." Bone **23**(1): 59-66.

- Murakami, H., N. Takahashi, T. Sasaki, N. Udagawa, S. Tanaka, I. Nakamura, D. Zhang, A. Barbier and T. Suda (1995). "A possible mechanism of the specific action of bisphosphonates on osteoclasts: tiludronate preferentially affects polarized osteoclasts having ruffled borders." Bone **17**: 137-144.
- Rhode, C., D. E. Anderson, A. L. Bertone and S. E. Weisbrode (2000). "Effects of phenylbutazone on bone activity and formation in horses." Am J Vet Res **61**(5): 537-543.
- Steiger, R. H., H. Geyer, A. Provencher, M. F. Perron-Lepage, B. von Salis and O. M. Lepage (1999). "Equine bone core biopsy: evaluation of collection sites using a new electric drilling machine." Equine Practice **21**: 14-21.
- Whitfield, C. T., M. J. Schoonover, T. C. Holbrook, M. E. Payton and K. M. Sippel (2016). "Quantitative assessment of two methods of tiludronate administration for the treatment of lameness caused by navicular syndrome in horses." Am J Vet Res **77**(2): 167-173.

CHAPTER 3.

INFLUENCE OF CLODRONATE ON BONE CELLS, MORPHOLOGY, REMODELING AND HEALING IN YOUNG HORSES

3.1 Introduction

Recently, the FDA approved the use of Clodronate disodium (Osphos, Dechra, Ltd., Staffordshire, UK) as a treatment for navicular disease in the horse (FOI, 2014). Clodronate is a non-nitrogen containing bisphosphonate that reduces osteoclastic bone resorption by causing osteoclast apoptosis (Lehenkari et al., 2002). Clodronate is similar to tiludronate, which has been used extensively to treat conditions associated with bone remodeling, such as navicular disease (Denoix et al., 2003, Whitfield et al., 2016) and tarsal osteoarthritis (Gough et al., 2010). However, unlike tiludronate, clodronate has been shown to have an analgesic effect by acting on glutamate and/or ATP-related pain transmission pathways (Shima et al., 2016). The Freedom of Information (FOI) Summary (FOI, 2014) reports on the clinical outcome in a group of horses diagnosed with navicular disease, treated with either clodronate or saline. At 56 days post-treatment, 68 of 86 clodronate-treated horses had improved by one score of the American Association of Equine Practitioner (AAEP) lameness scale, compared to 1 of 28 saline-treated horses (FOI, 2014). However, it is unclear whether the reduction in lameness in the aforementioned study (FOI, 2014) is due to clodronate treatment's effect on pathological bone remodeling, or its analgesic potential.

The FOI summary describes the effects of clodronate on bone mineral content, cortical bone strength and bone marrow evaluation evaluated by radiographic photometry, mechanical testing and histopathology, respectively, in normal horses. They reported no difference in these parameters between treated and saline controls at

6 months (FOI, 2014). However, the methods regarding how bone density data were obtained were not stated, and given the poor sensitivity of radiographs to determine bone density (Moyad, 2003), it is uncertain whether there was or was not an effect on bone in this cohort. Despite its known effect on bone remodeling rates in other species, the effect of clodronate on bone healing, especially in the horse, is unclear. In animal models, clodronate has been found to not alter endochondral bone formation within the callus or epiphyseal plate of rats (Nyman et al., 1996, Madsen et al., 1998), but reports show conflicting alterations to callus and bone properties, including no changes in bone mineral density (Koivukangas et al., 2003), 30% increase in bone mineral density (Madsen et al., 1998), increased calcium content within the callus (Nyman et al., 1993) and decreased healing callus strength (Tarvainen et al., 1994). Recently, it has been shown that osteoclasts are a necessary component of efficient endochondral ossification during fracture repair in mice (Lin and O'Connor, 2016); therefore, it is possible that clodronate may impair normal bone healing in horses, which calls for careful consideration when used in a clinical setting.

Therefore, the purpose of this study is to evaluate the effect of clodronate on bone morphology, bony cells, bone remodeling, and bone healing in young horses. These evaluations were performed by obtaining bone biopsies of the tuber coxarum using an established technique (Mitchell et al., 2017), and evaluated through histomorphometry and microCT. To evaluate bone healing, subsequent biopsies were taken from the initial biopsy site, which served as a novel bone defect model in the horse. We hypothesized that clodronate would reduce osteoclast number and function,

resulting in increased bone volume and increased bone apposition, as well as increased bone formation after injury.

3.2 Materials and Methods

Study Design

The experimental protocol used for this study was approved by the Louisiana State University IACUC (Protocol #15-081). Nine clinically healthy Thoroughbred horses, aged two – four years of age, were used in the study. Horses were obtained through donation, and did not have a known medical history prior to inclusion within the herd at the institution's facility. However, all horses underwent at least a two-week washout period prior to enrollment in the current study. Horses were randomly assigned using a coin flip to either a treatment (n=5) or control (n=5) group. Sample sizes were determined based on donation availability, and all eligible horses were considered. Additionally, if eligible horses became available during the course of data collection, they were evaluated and included in order to maximize sample size. A coin flip was used to randomly assigned horses to a treatment group (i.e., clodronate or saline), and only the surgeon knew group assignments until subsequent statistical analyses on data collected were ready to be performed.

Bone biopsies were taken from each horse; a baseline biopsy at Day 0, and a contralateral (Day 60) and ipsilateral re-biopsy of the initial site (Day 60R) 60 days after treatment (Figure 3.1). The initial biopsy side was randomly selected via coin flip. Subsequent to the initial biopsy collection (Day 0), each horse was administered clodronate (1.8 mg/kg, via IM injection, with the total volume divided into three injection

locations), or equal volume of 0.9% saline. This dose and route of administration is standard in the field (FOI, 2014). Prior to the second biopsy collections, the fluorochrome label oxytetracycline (Vetrimycin 100, VetOne, Boise, ID, USA) was administered at Day 47 and Day 57 to detect bone remodeling parameters. At Day 60, two additional biopsies were collected using the same procedure. Analyses of all biopsies included microCT and histomorphometry evaluations for changes in bone morphology, remodeling rates, and bone healing.

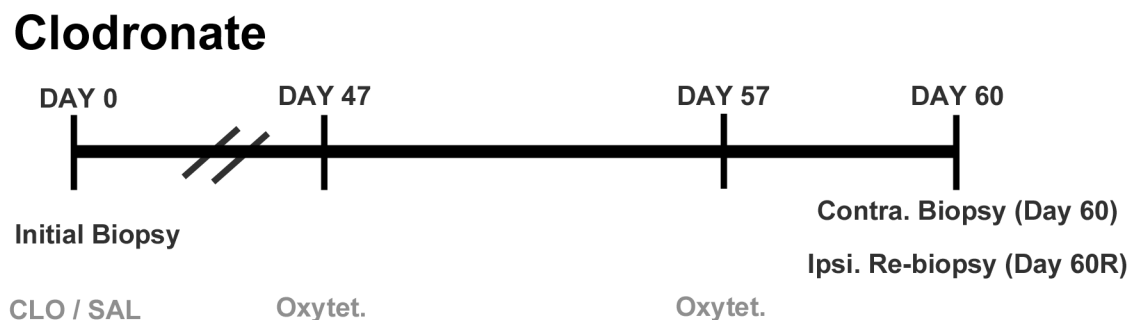


Figure 3.1 Clodronate study design schematic of time line, outlining biopsy collection and treatment administration. Abbreviations: Contra., Contralateral; Ipsi., Ipsilateral.

Study Horses

Thoroughbred horses were included for use in the study if they were clinically healthy and free from apparent musculoskeletal disease, determined through a physical examination, and were aged 3 to 4 years old (mean weight (\pm SD): 431.9 ± 52.4). Horses were housed individually in stalls following surgeries, and were returned to their respective group pastures after 24-48 hours post-operation, with free choice hay and water and grain twice daily.

Surgical Procedure & Treatment

The surgical methods utilized in this study have been previously published in detail (Mitchell et al., 2017). Briefly, surgeries were performed while horses were restrained in stocks and sedated with intravenous (IV) xylazine (Xylamed, Bimeda, Cambridge, ON, Canada) (0.35 to 0.5 mg/kg). A 10 cm by 10 cm square was centered over the palpable area of the tuber coxarum and was aseptically prepared. Local anesthetic (i.e., Lidocaine 2%, VetOne, Boise, ID, USA) was injected subcutaneously superficially down to the tuber coxarum periosteum, and horses were further sedated with detomidine hydrochloride (Dormosedan, Zoetis, Kalamazoo, MI, USA) (3 to 5 mg IV) and butorphanol tartrate (Torbugesic, Fort Dodge, New York, NY, USA) (3 to 5 mg IV)). A vertical incision was made over the tuber coxarum and was dissected to expose the cranial, caudal, deep and proximal margins. An oscillating saw was used to cut the proximal portion of the tuber coxarum, with constant saline lavage to limit thermal damage. After biopsy removal, the site was lavaged, and sutured closed (Mitchell et al., 2017). Flunixin meglumine (Prevail, Bimeda, Cambridge, ON, Canada) (1.1 mg/kg IV) was administered as an additional analgesic and the treatment (either clodronate or saline) was administered IM.

Following the initial biopsy, horses were stalled for 24-48 hours and monitored for signs of pain (Doherty and Valverde, 2006). Horses were returned to their group pastures and monitored daily for complications or lameness until sutures were removed 14 days later. At Day 47 and 57 post biopsy, the bone fluorescent label oxytetracycline (25 mg/kg) was administered slowly IV. Sixty days after the initial biopsy, two additional biopsies were collected; the contralateral side (Day 60 biopsy) and a re-biopsy of the

initial biopsy side (Day 60R biopsy) to evaluate bone healing. Biopsies were obtained using the same surgical methods as described above. However, careful consideration was made when placing the oscillating saw for the re-biopsy to ensure an adequately-sized biopsy of the tuber coxae was obtained without cutting into the pelvis. Surgical aftercare was identical.

MicroCT

Following biopsy collection, soft tissue was removed from tuber coxae samples, and biopsies were fixed in 10% non-buffered formalin for 7 days. After fixation, biopsies were stored in 70% ethanol at 20°C. For microCT (Scanco model 40, Scanco Medical AG, Basserdorf, Switzerland) evaluation, biopsies were placed in scanning holders with 70% ethanol, and scanned at 55kV, 0.3-second integration time, with a 30 µm voxel size in plane and a 30 µm slice thickness. Trabecular bone was selected as the region of interest, and the proper segmentation threshold was determined and used throughout for all samples. Trabecular bone was evaluated for bone volume (BV), total volume (TV), BV/TV, tissue mineral density, trabecular number (Tb.N), trabecular thickness (Tb.Th), trabecular spacing (Tb.Sp), connectivity density (Con.D), and structural model index (SMI) based on established procedures and nomenclature (Bouxsein et al., 2010).

Histology

After microCT evaluation, biopsies were prepared for histology as previously published (Mitchell et al., 2017). Day 0 and Day 60R biopsies were prepared for decalcified histology, and Day 60 biopsies were prepared for undecalcified histology so

visualization of fluorochrome labels was possible. Overall, histological preparation of biopsies differed slightly due to preparation technique required and the necessary size of the histologic slides. However, careful considerations were made to ensure sections of each biopsy were taken from the same location and plane of section. Day 0 and Day 60R biopsies were decalcified with 10% ethylenediaminetetraacetic acid (EDTA) and prepared for routine paraffin embedding. Day 0 and Day 60R biopsies were split in half and embedded separately, resulting in 6 – 8, 4 μm thick sections per biopsy, and were stained with hematoxylin and eosin (H&E). Day 60 biopsies were prepared intact for routine undecalcified histology, producing two, 45-60 μm thick sections. One section was stained with Stevenel's Blue and Van Gieson's picro fusion to evaluate bony cells and bone morphology via static histomorphometry, and the other section was left unstained for evaluation of bone remodeling via dynamic histomorphometry.

Histomorphometry evaluations were performed using standard software (Osteomeasure© Bone Histomorphometry System, Osteometrics, Inc., Decatur, GA, USA) following standard procedures and nomenclature (Dempster et al., 2013). Static histomorphometry parameters included direct measurements of: BV, marrow volume (Ma.V), bone surface (Crook et al.), eroded surface (ES), osteoblast surface (Ob.S), osteoblast number (Ob.N), osteoclast number (Oc.N), and osteoclast surface (Oc.S). Indirect static histomorphometry measurements included: Tb.N, Tb.Th, Tb.Sp, and the direct measurements list above standardized to respective areas and volumes. Dynamic histomorphometry parameters included mineralizing surface per BS (MS/BS), mineral apposition rate (MAR) and the bone formation rate per BS (BFR/BS).

Statistics

To evaluate the effect of clodronate, microCT and histomorphometry data were analyzed using independent analyses between treatment groups, as well as dependent analyses between biopsies (Figure 3.2). Prior to statistical comparisons, data were tested for normality using the Shapiro-Wilk test. Depending on normality, either parametric or non-parametric analyses were used for each parameter (i.e., paired Student's t-test, related samples Wilcoxon signed rank test, independent Student's t-test or independent samples Mann-Whitney U test). A related-sample test was used to evaluate changes from Day 0 biopsy to Day 60 biopsy, or Day 0 biopsy to Day 60R, within the control or treated horses. An unrelated-sample test was performed to evaluate difference between treated and control horses within Day 60 biopsy or Day 60R biopsy. Statistical analyses were performed using commercially-available software (SPSS, version 24, IBM Corporation, Armonk, New York, USA), and p-values of <0.05 were considered significant. If a parameter was significant but not normalized to respective biopsy size measurements, it was not reported (e.g., BV versus BV/TV). Due to the aforementioned issues with obtaining microCT data from two Day 0 biopsies, all data from those horses were excluded from dependent analyses.

3.3 Results

Surgical Technique

One horse (control group) was lost during the study and was euthanized due to reasons unrelated to the study, and was therefore not included in subsequent analyses.

Independent Analyses

Treated Horses vs Control Horses

Day 0 vs Day 0
Day 60 vs Day 60
Day 60R vs Day 60R

Dependent Analyses

Control Horses

Day 0 vs Day 60
Day 0 vs Day 60R

Treated Horses

Day 0 vs Day 60
Day 0 vs Day 60R

Figure 3.2 Schematic of statistical comparisons for microCT and histomorphometry data.

Horses received between 660 – 800 mg (mean \pm SD, 783.0 \pm 81.8 mg) of clodronate based on weight. All surgeries were successful in obtaining adequately-sized bone biopsies during each attempt, with no horses showing post-surgical lameness or complications. Day 0, Day 60 and Day 60R biopsies had a mean (\pm SD) TV of 1731 \pm 78, 1467 \pm 453 and 1080 \pm 646 mm³, respectively.

Bone Morphology

Due to technical difficulties, microCT analyses were only performed on three of the five Day 0 biopsies from the treated group. When comparing data from treated horses to control horses within the Day 60 biopsy, there was no significant effect of clodronate treatment on any of the 19 total bone morphology parameters as evaluated

by microCT (Figure 3.3). Similarly, there were no significant changes in bone morphology parameters between Day 0 and Day 60 biopsies within treated horses, or within control horses, as evaluated by MicroCT.

When comparing Day 0 biopsy to Day 60 biopsy within the control horses, several histomorphological parameters were significantly different: Day 0 biopsy was significantly greater than Day 60 biopsy in BV/TV ($p=0.02$) (Figure 3.3), and Oc.S/BS ($p=0.04$), and Day 60 biopsy was greater than Day 0 biopsy in Tb.Sp ($p=0.01$) and Ma.V/TV ($p=0.02$). When making the same comparison within treated horses, Day 0 biopsy was greater than Day 60 biopsy in Void Surface/BS ($p=0.049$), and Ob.N/TA ($p=0.03$) (Table 1), and Day 60 biopsy was greater than Day 0 biopsy in Ob.N/Ob.Perimeter ($p=0.02$). Overall, changes from Day 0 to Day 60 within control horses affected three out of 20 bone morphology parameters, and one out of 10 bone resorption parameters. Changes from Day 0 to Day 60 within treated horses showed differences in one out of 20 bone morphology parameters, and two out of 20 bone formation parameters.

Bone Remodeling

After 60 days, clodronate did not significantly alter any of the 14 bone remodeling parameters evaluated via dynamic histomorphometry (Figure 3.3).

Bone Healing

When comparing treated horses to control horses within the Day 60R biopsy, there was no significant effect of clodronate on any of the 19 bone morphology

parameters, as evaluated by microCT. Comparing Day 0 biopsy to Day 60R biopsy within control horses and then again within treated horses, there were no significant differences in any of the 19 bone morphology parameters evaluated via microCT.

When comparing Day 0 to Day 60R within control horses, the Day 60R biopsy had significantly higher ES/BS ($p=0.049$). Comparing Day 0 biopsy to Day 60R biopsy within treated horses, the same effect in ES/BS ($p=0.03$) was observed. Comparing treated horses to control horses within the Day 60R biopsy, treated horses had significantly higher BS/TV ($p=0.02$) and Tb.N ($p=0.02$), and significantly less Ob.S/BS ($p=0.04$). Overall, two out of 20 bone morphology parameters and one out of 20 bone formation parameters were significantly affected.

3.4 Discussion

This study details the effect of a single dose of clodronate on bone cells, morphology, remodeling, and healing in 5 healthy, young Thoroughbred horses. This is the first study that has evaluated bony changes due to clodronate in the horse, despite its prolific use in veterinary clinics. Additionally, clodronate's effect in horses under 4 years of age has not been determined. Overall, the data presented here demonstrates that overall there were no effects of clodronate after 60 days on bone morphology or remodeling when compared to the control group and when compared to baseline biopsies from the same horse, using the prescribed dose and route of administration.

Saline	MicroCT				Static Histomorphometry				Dynamic Histomorphometry	
	Day 0		Day 60	Day 60R	Day 0		Day 60	Day 60R	Day 60	
	BV/TV (%)	0.31 ± 0.04	0.32 ± 0.03	0.36 ± 0.17	BV/TV (%)	30.6 ± 7.5 ^a	21.2 ± 5.7 ^a	33.0 ± 15.7	sL.S/BS (%)	22.6 ± 4.5
	TbTh (mm)	0.16 ± 0.01	0.17 ± 0.01	0.20 ± 0.07	Ob.N/TA (/mm ²)	112.8 ± 73.6	53.9 ± 18.6	72.5 ± 22.1	dL.S/BS (%)	3.6 ± 2.6
	TbN (/mm)	1.8 ± 0.2	1.9 ± 0.3	1.9 ± 0.4	Oc.N/TA (/mm ²)	0.33 ± 0.27	0.01 ± 0.02	1.00 ± 0.75	MAR (µm/d)	1.16 ± 0.29
	ConDen (/mm ³)	8.0 ± 2.2	8.8 ± 3.0	9.1 ± 3.4					BFR/BV (%/yr)	203 ± 186

Clodronate	MicroCT				Static Histomorphometry				Dynamic Histomorphometry	
	Day 0		Day 60	Day 60R	Day 0		Day 60	Day 60R	Day 60	
	BV/TV (%)	0.32 ± 0.04	0.32 ± 0.03	0.40 ± 0.11	BV/TV (%)	30.7 ± 3.9	23.4 ± 4.8	34.5 ± 9.4	sL.S/BS (%)	28.4 ± 19.0
	TbTh (mm)	0.15 ± 0.02	0.16 ± 0.01	0.20 ± 0.04	Ob.N/TA (/mm ²)	88.3 ± 32.5 ^b	49.6 ± 16.0 ^b	63.4 ± 17.6	dL.S/BS (%)	4.3 ± 4.6
	TbN (/mm)	2.0 ± 0.1	1.9 ± 0.2	2.2 ± 0.2	Oc.N/TA (/mm ²)	0.44 ± 0.61	0.04 ± 0.05	0.84 ± 0.40	MAR (µm/d)	1.02 ± 0.29
	ConDen (/mm ³)	9.7 ± 1.0	8.6 ± 1.8	13.5 ± 3.0					BFR/BV (%/yr)	189 ± 178

Figure 3.3 Summary data (mean ± SD) of bone structure and remodeling parameters from Day 0, Day 60 and Day 60R biopsies for microCT, static histomorphometry and dynamic histomorphometry analyses in control (n=4) and treated (n=5) horses. Abbreviations: BV/TV, bone volume fraction (bone volume/total volume); Tb.Th, trabecular thickness; Tb.N trabecular number; Con.D, connectivity density; Ob.N/TA, number of osteoblasts per tissue area; Oc.N/TA, number of osteoclasts per tissue area; sL.S/BS, single label surface per bone surface; dL.S/BS, double label surface per bone surface; MAR, mineral apposition rate; BFR/BV, rate of bone formation (bone formation rate per unit of bone volume).^{a,b}Significant (P ≤ 0.05) difference between values with the same letter superscript. P-value results from paired Student's t-test. * Sample size for treated Day 0 biopsies contains 3 horses for microCT analysis.

One limitation to the current study is a lack of evaluation in a model of pathological bone remodeling, and a lack of clinical evaluations on lameness. However, a barrier to the field is that there is currently no data regarding whether clodronate does or does not affect bone remodeling in the horse at the doses administered. It is well known that bisphosphonates are powerful modifiers of the bone remodeling process, including in normal bone (Mashiba et al., 2005). Therefore, it is hypothesized that if there were a systemic effect of clodronate administration in the horse at the routine clinical dose administered, it would have been detected in the current study. As outlined above, treatment success in the previous study (FOI, 2014) may have been based on clodronate's pain-minimizing properties, and not due to changes in bone remodeling. This would explain the treatment success demonstrated in that clinical trial (FOI, 2014), but support the lack of bony changes shown in this study. However, a novel aspect of the current study is the evaluation of the effect of clodronate on bone healing secondary to a bone defect (i.e., the biopsy). Bone healing during clodronate use has been evaluated in rats (Madsen et al., 1998, Koivukangas et al., 2003), with no reports of adverse effects on bone remodeling (Koivukangas et al., 2003), but conflicting results on bone callus formation during fracture repair (Nyman et al., 1993, Nyman et al., 1996, Madsen et al., 1998). In this study, although not specifically evaluating fracture repair, we too found minimal effects on bone healing after injury.

The biopsy location, the tuber coxarum, used in the current study may not be representative of normal bone remodeling throughout the equine skeleton. However, previous work has shown that tiludronate, a bisphosphonate similar in structure and pharmacokinetics to clodronate (Lin, 1996), has been shown to accumulate in the bone

at highest concentrations within tuber coxae (Delguste et al., 2011). Thusly, while no such data exists for clodronate, given the similarities between tiludronate and clodronate, the tuber coxae are assumed to accumulate high concentrations. Similarly, the tuber coxae do not experience the same specific biomechanics experienced in the equine distal limb, specifically the navicular bone. It is possible that exercise may influence the effect of bisphosphonates on bone remodeling. Using the tuber coxae is a potential limitation in regards to conclusions about weight-bearing bones, given that clodronate is indicated for treatment of abnormal bone remodeling that primarily occurs in the distal limb in horses. However, bisphosphonates have been repeatedly shown to have systemic effects on bone (Drake and Cremers, 2010), especially trabecular bone (Pataki et al., 1997), so it can be reasonably argued that any changes that would occur secondary to treatment with clodronate would be identified in the selected biopsy location. Similarly, the pelvis has been identified as a location that can accurately represent changes found in weight bearing regions of the skeleton, such as the vertebrae (Mashiba et al., 2005).

While some significant differences in bone morphology were identified histologically, these changes were not confirmed via microCT, which represents a comprehensive evaluation of bone structure in three dimensions, as compared to two-dimensional histological assessments. While histomorphometry is excellent tool for cell and remodeling analyses of a slice of the total biopsy, microCT accounts for the entire biopsy volume. Therefore, despite small differences reported, the authors conclude that overall effects of clodronate on bone morphology and remodeling were insignificant in young horses after 60 days. Overall, there were small differences noted between

clodronate and saline comparisons. However, these differences were minor, and do not make biological sense as a stand-alone parameter in the broad overview of bone formation and resorption. It is possible that the changes seen in the control group are normal bony changes for this time frame, and clodronate preventing these changes from occurring in the treated group. However, as the changes reported are not consistent with overall changes expected. The low sample size may have limited the overall power of our analyses, but given the known efficacy of clodronate in other species on altering bone resorption (Minaire et al., 1986), even a small difference, if present, was expected to be observed. The 60 day duration of this study is short; however this duration has been used in other studies examining bone remodeling (Rohde et al., 2000) and is associated with clinical improvement of lameness in the majority of horses treated with either clodronate or tiludronate (Denoix et al., 2003, Gough et al., 2010, FOI, 2014). Clinical improvement in lameness may not be related to changes in bone morphology or remodeling, but without investigating the effects in normal horses, pathologic changes or responses following therapy will be harder to identify. Additionally, our study utilized both internal controls and a separate control group, and found no additional differences in any parameter using these comparisons. However, future evaluations should utilize a larger sample size to increase power to determine if clodronate has minimal effect on bone remodeling.

In conclusion, we found that clodronate has no effect on bone morphology, as evaluated via microCT, and no effect on bone remodeling after 60 days in young horses. There were minimal effects found via static histomorphology; however, these results are insignificant in the absence of microCT data and other normalized

parameters. Additionally, we determined that clodronate does not negatively affect bone healing in the presence of a bone injury, in this skeletal location, after 60 days.

3.5 References

- Bouxsein, M. L., S. K. Boyd, B. A. Christiansen, R. E. Guldberg, K. J. Jepsen and R. Müller (2010). "Guidelines for assessment of bone microstructure in rodents using micro-computed tomography." J Bone Min Res **25**(7): 1468-1486.
- Crook, T. C., S. E. Cruickshank, C. M. McGowan, N. Stubbs, A. M. Wilson, E. Hodson-Tole and R. C. Payne (2010). "A comparison of the moment arms of pelvic limb muscles in horses bred for acceleration (Quarter Horse) and endurance (Arab)." J Anat **217**(1): 26-37.
- Delguste, C., M. Doucet, A. Gabriel, J. Guyonnet, O. M. Lepage and H. Amory (2011). "Assessment of a bone biopsy technique for measuring tiludronate in horses: a preliminary study." Can J Vet Res **75**(2): 128-133.
- Dempster, D. W., J. E. Compston, M. K. Drezner, F. H. Glorieux, J. A. Kanis, H. Malluche, P. J. Meunier, S. M. Ott, R. R. Recker and A. M. Parfitt (2013). "Standardized nomenclature, symbols, and units for bone histomorphometry: a 2012 update of the report of the ASBMR Histomorphometry Nomenclature committee." J Bone Miner Res **28**(1): 1-16.
- Denoix, J. M., D. Thibaud and B. Riccio (2003). "Tiludronate as a new therapeutic agent in the treatment of navicular disease: a double-blind placebo-controlled clinical trial." Equine Vet J **34**(4): 407-413.
- Doherty, T. and A. Valverde (2006). Manual of equine anaesthesia and analgesia, Blackwell Publishing.
- Drake, M. T. and S. Cremers (2010). "Bisphosphonate therapeutics in bone disease: the hard and soft data on osteoclast inhibition." Mol Interv **10**(3): 141.
- FOI. (2014). "Freedom of Information Summary: For the control of clinical signs associated with navicular syndrome in horses.", from <https://www.fda.gov/downloads/AnimalVeterinary/Products/ApprovedAnimalDrugProducts/FOIADrugSummaries/UCM406997.pdf>.
- Gough, M. R., D. Thibaud and R. K. W. Smith (2010). "Tiludronate infusion in the treatment of bone spavin: a double blind placebo-controlled trial." Equine Vet J **42**(5): 381-387.
- Koivukangas, A., J. Tuukkanen, K. Kippo, T. Jamsa, R. Hannuniemi, I. Pasanen, K. Vaananen and P. Jalovaara (2003). "Long-term administration of clodronate does not prevent fracture healing in rats." Clin Orthop Relat Res **408**: 268-278.

- Lehenkari, P. P., M. Kellinsalmi, J. P. Näpänkangas, K. V. Ylitalo, J. Mönkkönen, M. J. Rogers, A. Azhayev, K. H. Väänänen and I. E. Hassinen (2002). "Further insight into mechanism of action of clodronate: inhibition of mitochondrial ADP/ATP translocase by a nonhydrolyzable, adenine-containing metabolite." Mol Pharmacol **61**(5): 1255-1262.
- Lin, H. N. and J. P. O'Connor (2016). "Osteoclast depletion with clodronate liposomes delays fracture healing in mice." J Orthop Res.
- Lin, J. H. (1996). "Bisphosphonates: a review of their pharmacokinetic properties." Bone **18**(2): 75-85.
- Madsen, J. E., T. Berg-Larsen, O. J. Kirkeby, J. A. Falch and L. Nordsletten (1998). "No adverse effects of clodronate on fracture healing in rats." Acta Orthop Scand **69**(5): 532-536.
- Mashiba, T., S. Hui, C. H. Turner, S. Mori, C. C. Johnston and D. B. Burr (2005). "Bone Remodeling at the Iliac Crest Can Predict the Changes in Remodeling Dynamics, Microdamage Accumulation, and Mechanical Properties in the Lumbar Vertebrae of Dogs." Calcif Tissue Int **77**(3): 180-185.
- Mashiba, T., S. Mori, D. B. Burr, S. Komatsubara, Y. Cao, T. Manabe and H. Norimatsu (2005). "The effects of suppressed bone remodeling by bisphosphonates on microdamage accumulation and degree of mineralization in the cortical bone of dog rib." J Bone Miner Metab **23 Suppl**(S1): 36-42.
- Minaire, P., J. Depassio, E. Berard, P. Meunier, C. Edouard, G. Pilonchery and G. Goedert (1986). "Effects of clodronate on immobilization bone loss." Bone **8**: S63-68.
- Mitchell, C. F., H. A. Richbourg, B. A. Goupil, A. N. Gillett and M. A. McNulty (2017). "Assessment of tuber coxae bone biopsy in the standing horse." Vet Surg.
- Moyad, M. A. (2003). "Osteoporosis: a rapid review of risk factors and screening methods." Urol Oncol **21**: 375-379.
- Nyman, M. T., T. Gao and T. C. Lindholm (1996). "Healing of a tibial double osteotomy is modified by clodronate administration." Arch Orthop Trauma Surg **115**: 111-114.
- Nyman, M. T., P. Paavolainen and T. S. Lindholm (1993). "Clodronate increases the calcium content in fracture callus. An experimental study in rats." Arch Orthop Trauma Surg **112**(5): 228-231.
- Pataki, A., K. Müller, J. R. Green, Y. F. Ma, Q. N. Li and W. S. Jee (1997). "Effects of Short-Term Treatment With the Bisphosphonates Zoledronate and Pamidronate on Rat Bone: A Comparative Histomorphometric Study on the Cancellous Bone Formed Before, During, and After Treatment." Anat Rec **249**(4): 458-468.

- Rohde, C., D. E. Anderson, A. L. Bertone and S. E. Weisbrode (2000). "Effects of phenylbutazone on bone activity and formation in horses." Am J Vet Res **61**(5): 537-543.
- Shima, K., W. Nemoto, M. Tsuchiya, K. Tan-No, T. Takano-Yamamoto, S. Sugawara and Y. Endo (2016). "The Bisphosphonates Clodronate and Etidronate Exert Analgesic Effects by Acting on Glutamate- and/or ATP-Related Pain Transmission Pathways." Biol Pharm Bull **39**(5): 770-777.
- Tarvainen, R., H. Olkkonen, T. Nevalainen, P. Hyvonen, I. Arnala and E. Alhava (1994). "Effect of clodronate on fracture healing in denervated rats." Bone **15**(6): 701-705.
- Whitfield, C. T., M. J. Schoonover, T. C. Holbrook, M. E. Payton and K. M. Sippel (2016). "Quantitative assessment of two methods of tiludronate administration for the treatment of lameness caused by navicular syndrome in horses." Am J Vet Res **77**(2): 167-173.

CHAPTER 4. ANATOMICAL VARIATION OF THE TARSUS IN COMMON INBRED MOUSE STRAINS²

4.1 Introduction

Rodent models are widely used in orthopedic and biomechanical research, which rely upon accurate knowledge of the anatomy of the hind limb (Gillis and Biewener, 2001, Settle et al., 2003, Glasson et al., 2007, Rose et al., 2013, Banzrai et al., 2016). Their small size, fully sequenced genome (Corsortium et al., 2002, Adams et al., 2015) and short lifespan make them a common candidate for translational studies related to human disease. Therefore, detailed and accurate anatomical descriptions are extremely important for any translational research that involves the musculoskeletal system of rodents. Prior to the advent of novel technologies that allow advanced imaging of various tissues and organ systems, scientists relied on artistic interpretations of anatomy (Cook, 1965, Rugh, 1968, Popesko et al., 1992) for references. These drawings are still used today as anatomical references for research and education. These references describe the tarsal anatomy of mice (*Mus musculus*) as having eight bones, including tarsal bones I (*os tarsale I*), II (*os tarsale II*), III (*os tarsale III*) and IV (*os tarsale IV*), medial tibial (*tibiale mediale*), central (*os tarsi centrale*), calcaneus and talus (Cook, 1965, Rugh, 1968). The anatomy of the murine tarsus, as described by Cook (Cook, 1965) and Rugh (Rugh, 1968), is identical to the anatomy found in the rat (Popesko et al., 1992).

² This chapter previously appeared as Richbourg, H. A. et al. Anatomical Variation of the Tarsus in Common Inbred Mouse Strains. *Anat Rec* (2016) DOI: 10.1002/ar.23493. Reprinted by permission of John Wiley and Sons via RightsLink.

While useful, these conventional references do not depict three-dimensional (3D) relationships between anatomical structures. Published anatomical descriptions have expanded to include high resolution, 3D images and models of anatomy derived from computed tomography (Yakatan et al., 1982) scans from several species. The skeletal anatomy of a C57Bl/6 (Black6) laboratory mouse has been characterized in extensive detail by utilizing microCT (Bab et al., 2007), and conflicting data describing murine tarsal anatomy has been observed between the established anatomical illustrations (Cook, 1965, Rugh, 1968) and the more recent text (Bab et al., 2007) that uses microCT to describe murine skeletal anatomy. When examining the tarsus in high-resolution microCT scans of a 10-week-old male Black6 laboratory mouse (Bab et al., 2007), the central tarsal bone and tarsal bone III are fused; however, this fused bone is labeled as the navicular bone (i.e. central tarsal bone) with no discussion on the absence of the tarsal bone III. Additionally, Duce et al. (Duce et al., 2010) reported difficulty in determining the interface between the central and tarsal bone III in Black6 mice during digital segmentation of micro-magnetic resonance imaging (MRI) data.

Normal variation in tarsal bone anatomy has been documented in several other species, both domestic and exotic (Shubin et al., 1995, Dyce et al., 2010). Although normal variation in ossification patterns within rodents has been documented (Wilson et al., 2010), normal variations in tarsal anatomy within mice remain undocumented. This lack of knowledge impacts studies that have identified abnormalities of the tarsus in mice afflicted with mutations affecting the expression of growth and differentiation factors (GDF) 5 and 6 (Grüneberg and Lee, 1973, Storm et al., 1994, Settle et al., 2003, Tassabehji et al., 2008). One of these mutations is characterized as brachypodism, a

disease that is caused by a recessive gene mutation that affects the appendicular skeleton, resulting in shortened long bones and fusion of bones within the tarsus and carpus (Grüneberg and Lee, 1973, Storm et al., 1994, Seemann et al., 2005). In these studies, the fusion of tarsal bone III and the central tarsal bone is represented as an abnormal consequence of gene mutations in commonly used inbred laboratory mouse strains. Due to conflicting information between these studies and anatomical references, documenting the detailed anatomy of the tarsal anatomy in mice is important for future work involving the skeletal structures in this region. Therefore, the purpose of the current study is to characterize the normal anatomy of the tarsus and to clarify the presence and number of bones within this region in normal laboratory mice, evaluating both young and mature individuals of multiple lineages. To determine the phylogenetic extent of the potentially derived tarsal anatomy observed in laboratory mice, they are compared with other closely related murines by evaluating the rat (*Rattus norvegicus*); and a member of Cricetidae as the outgroup, the more distantly related white-footed mouse (*Peromyscus leucopus*) (Blanga-Kanfi et al., 2009).

4.2 Materials and Methods

Study Design

Left hind limbs from 17 laboratory mice, 2 white-footed mice and 5 rats were collected. To accurately determine variation in hind limb bony anatomy, tarsi from these specimens were analyzed via high-resolution microCT. Three-dimensional reconstructions of the tarsal bone anatomy were then made for comparisons as outlined below. In addition, decalcified histology of the tarsus from the hind limb of one Black6

laboratory mouse and one BalbC laboratory mouse was analyzed to confirm tarsal bone fusion.

Specimens

All specimens in this study were collected post-mortem as discarded tissues under approved IACUC protocols, and were not included in concurrent studies involving musculoskeletal disease before euthanasia. Details regarding the specimens utilized in the study are outlined in Figure 4.1. In short, two laboratory strains of mice (*M. musculus*; Black6, n=15; and BalbC, n=2), white-footed mice (*P. leucopus*, n=2) and laboratory rats (*R. norvegicus*, Sprague Dawley, n=5) were evaluated. Within the Black6 inbred laboratory mice, hind limbs from mice of various ages were included: 24 weeks (n=7), 16 weeks (n=3), 11 weeks (n=3), 8 weeks (n=1) and 3.5 weeks (n=1). The left hind limb from each specimen was disarticulated at the coxofemoral joint and fixed in 10% neutral-buffered formalin prior to analysis.

Micro-computed tomography and 3D reconstruction

Samples were scanned (Scanco Model 40, Scanco Medical AG, Basserdorf, Switzerland) in 70% ethanol at 55 kV, 145 μ A with various isotropic voxel resolutions (outlined in Table 4.1) due to limb size. The region of interest (Bouxsein et al., 2010) for microCT scanning included the region between the distal tibia to the proximal metatarsal bones. Each scan was exported as a set of DICOM files and imported to the

Specimen Characteristics						
Common Name	Species	Strain	Age	Sex	n	Resolution
Laboratory Mouse	<i>M. muscus</i>	C57Bl/6	11 wks	F	3	16 μ m
	<i>M. muscus</i>	C57Bl/6	16 wks	F	3	16 μ m
	<i>M. muscus</i>	C57Bl/6	24 wks	F	7	16 μ m
	<i>M. muscus</i>	C57Bl/6	8 wks	F	1	12 μ m
	<i>M. muscus</i>	C57Bl/6	3 wks	F	1	12 μ m
	<i>M. muscus</i>	BalbC	12 wks	F	2	16 μ m
White-Footed Mouse	<i>P. leucopus</i>		Immature	M	1	12 μ m
			Mature	M	1	12 μ m
Laboratory Rat	<i>R. norvegicus</i>	Sprague Dawley	12 wks	F	3	16 μ m
	<i>R. norvegicus</i>	Sprague Dawley	52 wks	M	1	20 μ m
	<i>R. norvegicus</i>	Sprague Dawley	104 wks	M	1	20 μ m

Figure 4.1 Characteristics for study samples utilized, including common name, species name, specific strain (if applicable), age (if known), sex, the number of samples per category and the microCT scanning resolution. Exact ages are not known for animals obtained from the field, so maturation was deduced based on closure of physes within the hind limb. For age reference, sexual maturity of the mouse and rat is estimated to be as early as 4 to 5 weeks.

imaging software Amira version 6.0.1 (FEI Software, Hillsboro, OR, USA). Anatomical features were segmented by hand, using a Wacom Intuos Pro large tablet (Wacom Technology Corp., Vancouver, WA, USA). Standard veterinary anatomical nomenclature was utilized throughout the study (Nomenclature, 2012).

Histology

Following microCT scanning, a representative hind limb from one Black6 and BalbC laboratory mouse were prepared for routine decalcified histology. The hind limbs were decalcified in 10% ethylenediaminetetraacetic acid (EDTA) for two weeks, processed, embedded intact into paraffin and serially sectioned in the sagittal plane. Four to five representative sections were selected through the central tarsal region, ensuring inclusion of the central tarsal bone and tarsal bone III, and stained with hematoxylin & eosin (H&E). Sections were evaluated for presence of joint space, hyaline cartilage and/or subchondral bone.

4.3 Results

MicroCT and Digital Models

The laboratory mouse tarsus has seven individual tarsal bones: the calcaneus, talus, fused central and tarsal bone III, medial tibial bone and tarsal bones I, II, and IV (Figure 4.2). The tibia and fibula articulate distally with the talus, and the tarsocrural joint incorporates the distal tibia and fibula, talus and calcaneus. The proximal row of tarsal bones includes the medial tibial bone, talus and calcaneus. The talus articulates with the calcaneus caudally, medial tibial bone medially and the fused central and tarsal bone III distally. The middle row of tarsal bones is composed of the proximal portion of tarsal bone I, proximal portion of the fused central and tarsal bone III and tarsal bone IV (medial to lateral), and the distal row consists of the distal portion of tarsal bone I, tarsal bone II, distal portion of the fused central and tarsal bone III and the distal portion of tarsal bone IV (medial to lateral). The metatarsals are distal to the tarsal bones,

consisting of (medial to lateral) metatarsals I, II, III, IV, and V. Each metatarsal bone articulates with the corresponding tarsal bone (i.e., metatarsal I articulates with tarsal bone I), with the exception of metatarsal V, which articulates with the distal portion of tarsal IV. Metatarsal V protrudes the furthest proximally of the metatarsals.

In contrast, the rat and white-footed mouse have a separate central tarsal bone and tarsal bone III (Figure 4.2), consisting of 8 separate tarsal bones (full pes shown in Figure 4.3). Two-dimensional slices from microCT scans confirm fusion of the central and tarsal bone III in both strains of laboratory mice, and separation in the rat (Figure 4.4). In this particular white-footed mouse specimen, metaphyseal physes were not ossified in the proximal and distal tibia, proximal and distal fibula, proximal metatarsal I and metatarsal V; in addition, the apophysis that gives rise to the tuber calcanei was not ossified, indicating that this specimen was skeletally immature. Similar to the white-footed mouse, metaphyseal physes were not ossified in the tibia, fibula and metatarsal I in the 3-week- old Black6, and the fibula in the 8-week-old Black6. Similarly, the apophysis that gives rise to the tuber calcanei was not ossified in the 3- and 8-week-old specimens. Comparative tarsal anatomy of the laboratory mouse, rat and white-footed mouse are shown in Figure 4.5.

Histology

Sagittal sections of the tarsus in both the adult Black6 and BalbC mice show a single, fused central and tarsal bone III (Figure 4.6). In both samples, a horizontal band of healthy hyaline cartilage was present near the approximated fusion site, but is surrounded by healthy and intact trabecular bone.

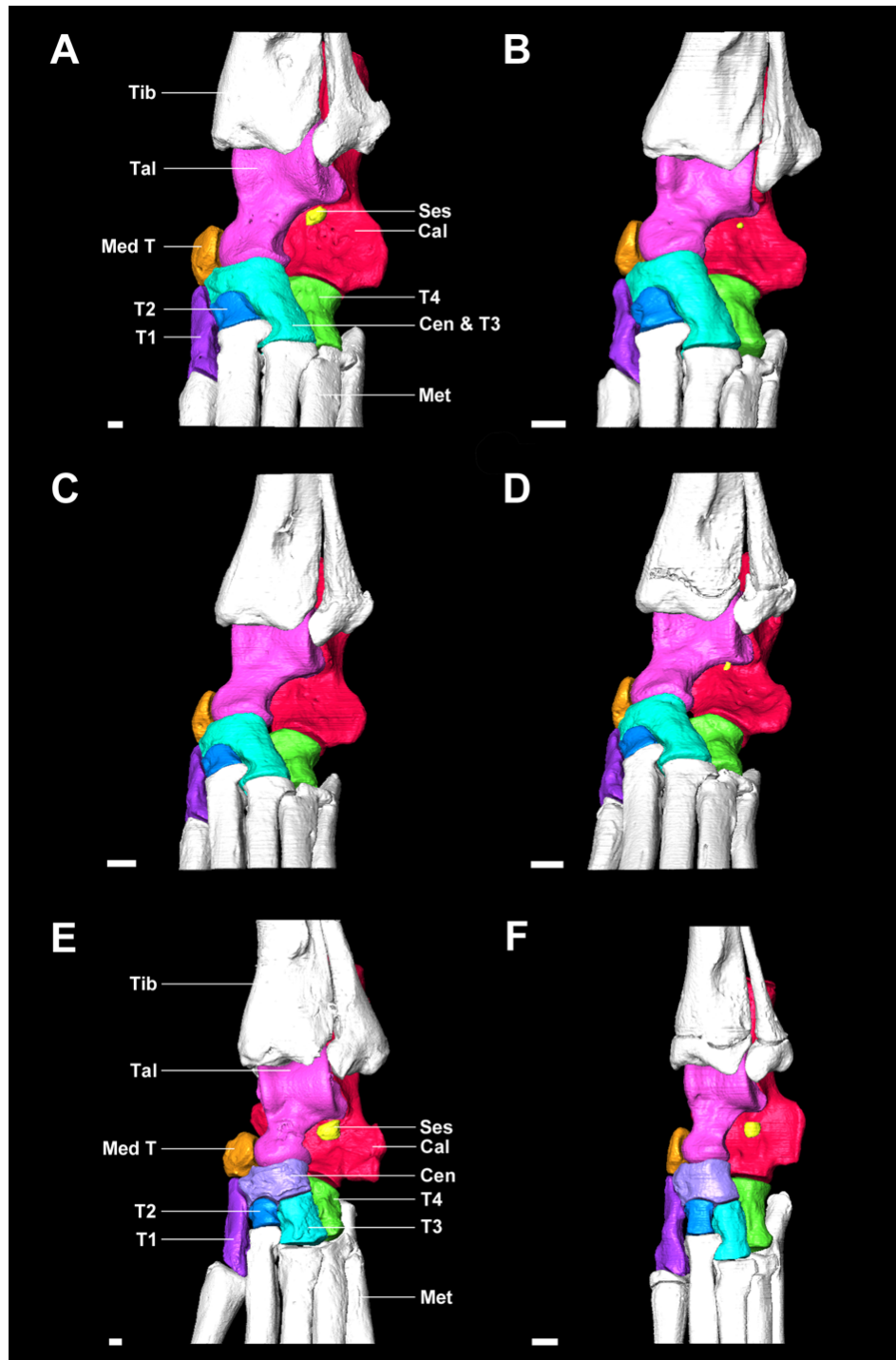


Figure 4.2 Representative 3D reconstructions of the left tarsus (cranial view) of A) adult Black6 mouse, B) adult BalbC mouse, C) 8 week old Black6 mouse, D) 3.5 week old Black6 mouse, E) rat, and F) white-footed mouse. Abbreviations: Cal, calcaneus; Cen, central tarsal bone; Cen & T3, fused central and tarsal bone III; Fib, fibula; Med T, medial tibial bone; Met, metatarsals; Ses, sesamoid; Tal, talus; Tib, tibia; T1, tarsal bone I; T2, tarsal bone II; T3, tarsal bone III; T4, tarsal bone IV. Scale bar = 0.5 mm.

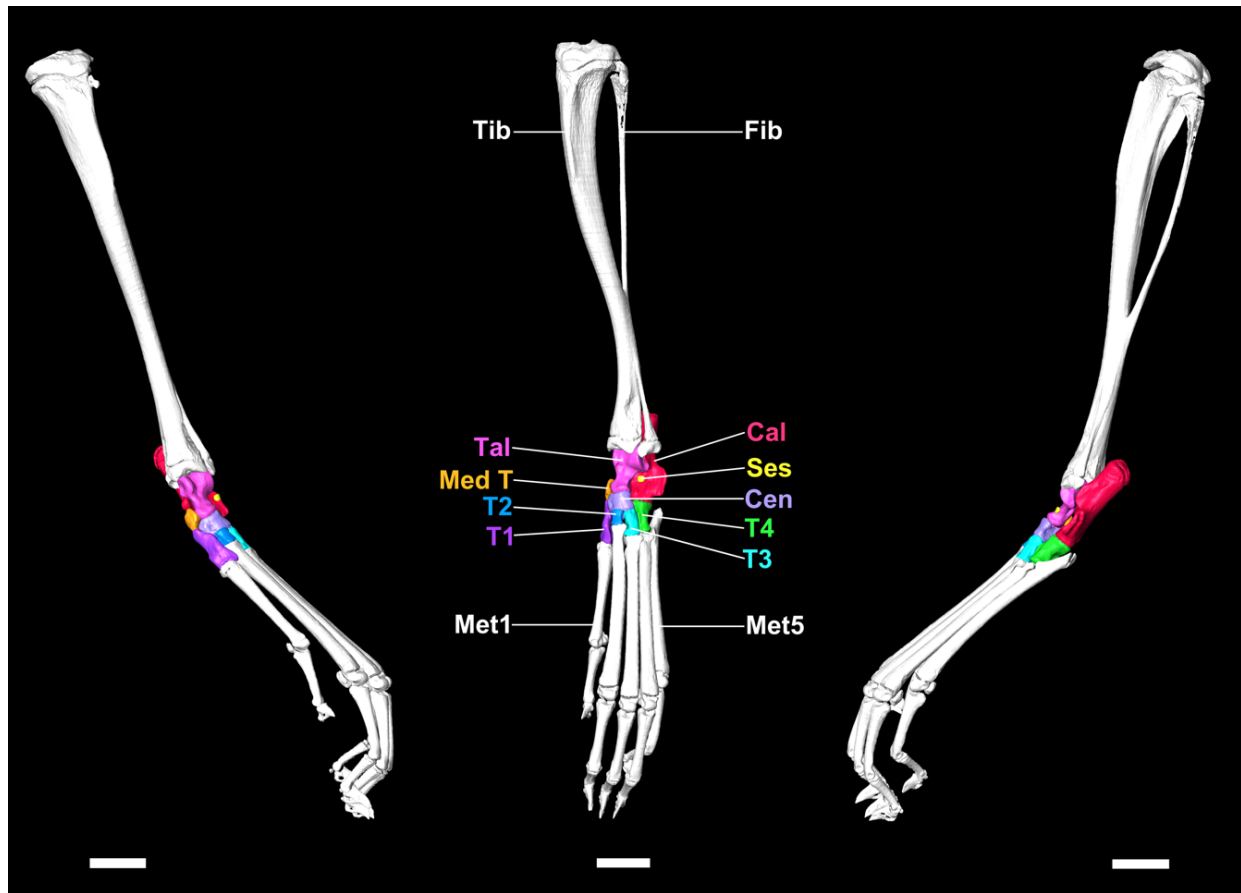


Figure 4.3 Three-dimensional reconstructions of the left pes of the white-footed mouse (*P. leucopus*) in medial, cranial and lateral view from left to right. Abbreviations: Cal, calcaneus; Cen, central tarsal bone; Fib, fibula; Med T, medial tibial bone; Met1, metatarsal I; Met5, metatarsal IV; Ses, sesamoid; Tal, talus; Tib, tibia; T1, tarsal bone I; T2, tarsal bone II; T3, tarsal bone III; T4, tarsal bone IV. Scale bar = 2.5 mm.

4.4 Discussion

In this study, we determined that the fusion of the central and tarsal bone III is present in both strains of laboratory mice examined. Considering that the fusion was present in all individuals of varying ages ($n=17$), we conclude this to be a ubiquitous tarsal characteristic in laboratory mice. In addition to microCT evaluations, histology further confirmed this fusion. Our findings contradict the majority of previously published data (Cook, 1965, Rugh, 1968, Popesko et al., 1992) but support the recent images

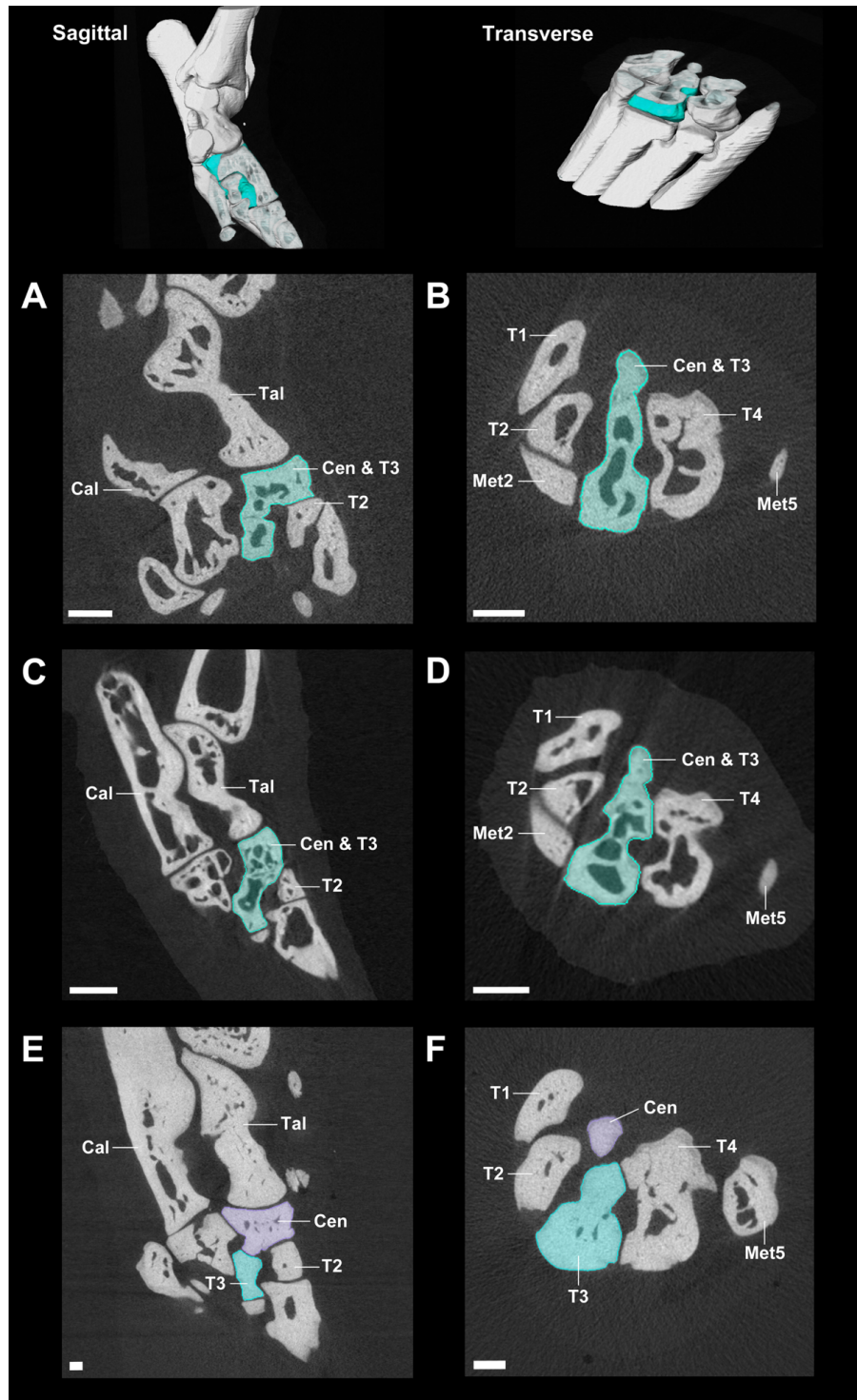


Figure 4.4 Representative sagittal (A, C, E) and transverse (B, D, F) slices from microCT scans showing the central (purple) and tarsal bone III (blue) in the adult Black6 mouse (A, B), adult BalbC mouse (C, D) and rat (E, F). Abbreviations: Tal, talus; Cal, calcaneus; Cen & T3, fused central and tarsal bone III; Cen, central; T1, tarsal bone I; T2, tarsal bone II; T3, tarsal bone III; T4, tarsal bone IV; Met2, metatarsal II; Met5, metatarsal V. Scale bar = 0.5 mm.

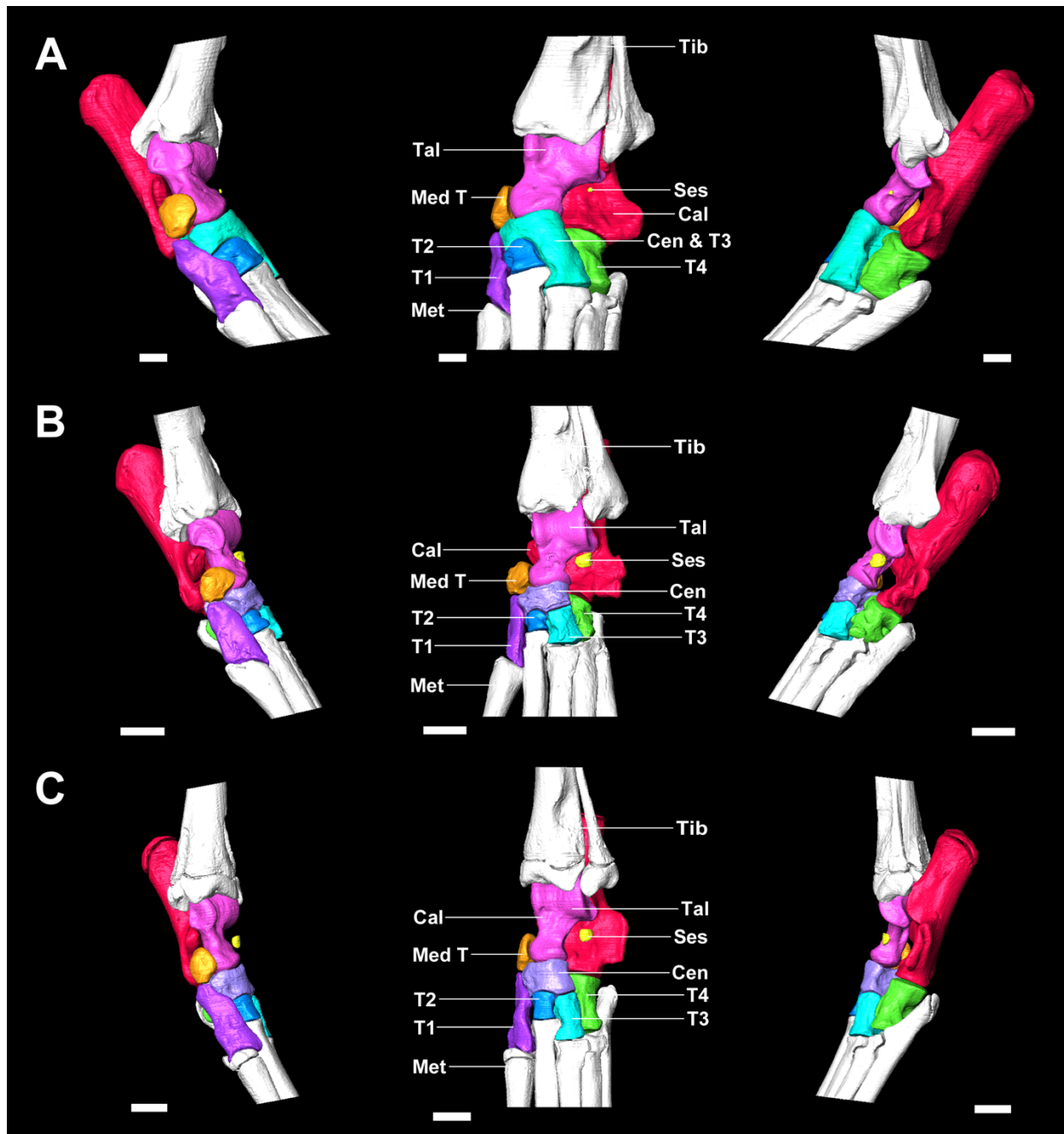


Figure 4.5 Three-dimensional reconstructions for comparative anatomy of the left pes of the A) adult BalbC mouse (*M. musculus*), B) rat (*R. norvegicus*), and C) white-footed mouse (*P. leucopus*) in medial, cranial and lateral view from left to right. Abbreviations: Tib, tibia and fibula; Tal, talus; Ses, sesamoid; Cal, calcaneus; Med T, medial tibial; Cen & T3, fused central and tarsal bone III; Cen, central; T1, tarsal bone I; T2, tarsal bone II; T3, tarsal bone III; T4, tarsal bone IV; Met, metatarsals. Scale bar = A) 0.5 mm, B) 2.5 mm, C) 1 mm.

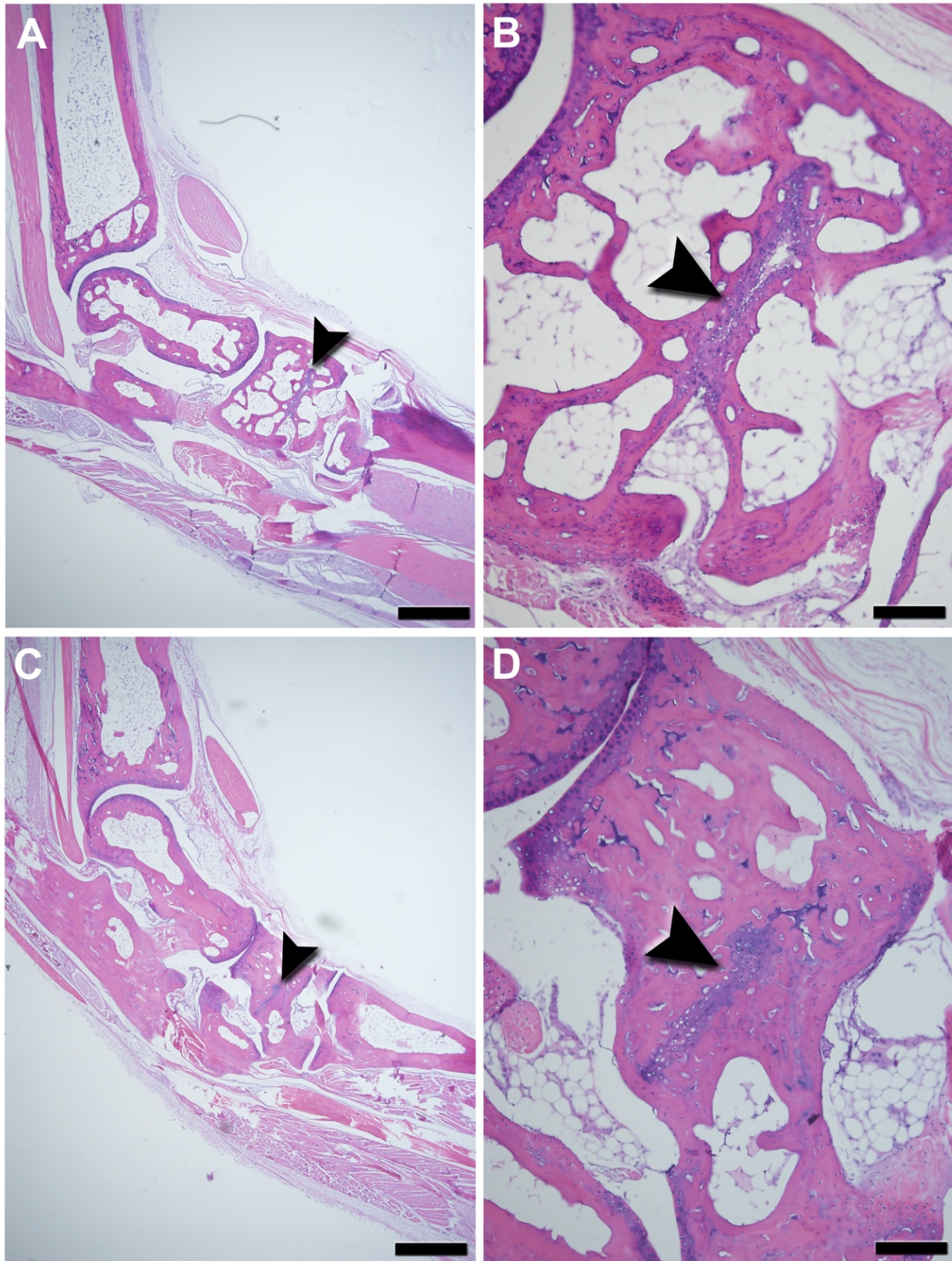


Figure 4.6 Decalcified H&E stained histologic sagittal sections from a representative adult BalbC mouse (A & B) and adult Black6 mouse (C & D). Arrowheads designate hyaline cartilage within the fused central and tarsal bone III. Scale bars = 500 μ m (A & C) and 100 μ m (B & D).

published by Bab et al. (Bab et al., 2007). This study further characterizes these differences in two strains of mice by comparing the laboratory mouse morphotype to the closely related rat and the more distant white-footed mouse. Due to the fact that the observed tarsal fusion was not present in the rat, we believe this fusion to be a recent development due to extensive selective breeding of laboratory mice, potentially expediting evolutionary changes. In addition, histological evaluations showed the presence of hyaline cartilage in both laboratory strains, demonstrating that the central bone and tarsal bone III were likely, at one point, two separate bones. The presence of cartilage could indicate that either the bone has completely fused and this is the remnant of the joint space, or the bone has only partially fused, and the presence of the cartilage surrounded within bone is simply an orientation limitation of a two-dimensional view. It is possible that this fusion could have occurred during normal postnatal growth and development, as studies evaluating bone development show these bones as being separate in young mice (Storm et al., 1994, Patton and Kaufman, 1995); however, our findings are somewhat contradictory, as we identified this fusion in mice as young as three weeks old. One limitation to our study was that only one laboratory mouse at three weeks of age was analyzed. A potential explanation for these anatomical differences could be the different laboratory mouse populations. The laboratory mice used in this study were either purchased from the Jackson Laboratory or bred on site.

Several studies have characterized the fusion of the central and tarsal bone III as an abnormal finding secondary to mutations associated with brachypodism (Storm et al., 1994). Storm et al. (Storm et al., 1994) found fusion of the central and tarsal bone III

in BalbC mice with null mutations in GDF5 during embryonic development. It is thought that disrupting various members of the bone morphogenic proteins (BMPs) may affect differentiation and separation of precursor bones within the carpus and tarsus (Storm et al., 1994). In contrast, our data demonstrate that fusion of the central and tarsal bone III is likely a normal maturation characteristic, and not a pathological finding as described (Grüneberg and Lee, 1973, Storm et al., 1994). Furthermore, if this fusion in the tarsal bones occurred as the result of a genetic mutation within the inbred laboratory mouse strains, it is possible that this change occurred during the 20-50 years since those studies were published, meaning that the normal mice included in those studies did indeed have separated tarsal bones. More recently, Duce et al. (Duce et al., 2010) reported difficulties distinguishing the boundaries of the central and tarsal bone III using micro-magnetic resonance imaging of Black6 mice. These difficulties could be explained by our results. Our findings directly impact these studies, as we have shown that this fusion is not a lesion secondary to disease, and is in fact a normal occurrence within two laboratory mouse strains.

The central and tarsal bone III in the white-footed mouse are unfused and remain two distinctly separate bones. It is possible that fusion could occur in a later phase of maturation of the white-footed mouse; however, this does not appear to be the case, as the laboratory mice with a similar epiphyseal plate status show fused tarsal bones. In addition, tarsal bones ossify with a single center of ossification during development (Patton and Kaufman, 1995), thus normal postnatal fusion of these two bones is unlikely. Differences in the white-footed mouse and a laboratory mouse may be due to differences in locomotion (i.e., semi-saltatorial versus scansorial) or due to their distant

phylogenetic relationship. In addition, only two white-footed mice were available for evaluation. Future studies would require further and more comprehensive analyses of the tarsal anatomy of wild typed mice of various ages for direct comparisons to the skeletal anatomy of their distant inbred relatives.

The absence of fusion in the closely-related rat shows that this fusion is specific to the laboratory mouse and is not an ancestral state. The fusion of the central bone and tarsal bone III is most likely the result of a genetic mutation from human-directed breeding; however, evaluations of a wild type *M. musculus* is necessary to determine if this fusion is only present in laboratory mice or also found in other populations. Although the mice used in this study are bred as control, wild type mice, they have still been subjected to inbreeding, and therefore may not reflect the true wild type state of mice.

Herein we were able to successfully show that fusion of the central and tarsal bone III is a normal characteristic in adults of two strains of inbred laboratory mice commonly used for orthopedic research, as well as characterize the tarsal anatomy for the white-footed mouse and rat. Although we guardedly apply this conclusion to all strains and populations of laboratory mice due to sample size, we believe these findings should be considered for studies requiring detailed knowledge of tarsal anatomy in these species. It is possible that there are biomechanical consequences of the fusion of the central and tarsal bone III; however, the fusion does not span the entire distal intertarsal joint, and therefore only limits range of motion in the center of the joint. Joint fusions are common in horses with distal intertarsal osteoarthritis, and after surgical fusion, horses return to athletic performance without hindrance on range-of-motion in the tarsus (Dechant et al., 2005). Therefore, although the fusion of the central and tarsal

bone III may limit the overall movement of the joint, it likely does not have major consequences on gait. Clarification of the timing of fusion should be evaluated through the investigation of additional stages, including embryogenesis, as studies evaluating the effects of GDF 5/6 mutations in tarsal anatomy evaluate developmental anatomy. In addition, older mice (i.e., >1 year of age) should also be evaluated to determine if the cartilage and joint space observed disappears, indicating that fusion is actively occurring later in life.

4.5 References

- Adams, D. J., A. G. Doran, J. Lilue and T. M. Keane (2015). "The Mouse Genomes Project: a repository of inbred laboratory mouse strain genomes." Mamm Genome **26**(9-10): 403-412.
- Bab, I. A., C. Hajbi-Yonissi, Y. Gabet and R. Müller (2007). Micro-tomographic atlas of the mouse skeleton, Springer Science & Business Media.
- Banzrai, C., H. Nodera, T. Kawarai, S. Higashi, R. Okada, A. Mori, Y. Shimatani, Y. Osaki and R. Kaji (2016). "Impaired Axonal Na(+) Current by Hindlimb Unloading: Implication for Disuse Neuromuscular Atrophy." Front Physiol **7**: 36.
- Blanga-Kanfi, S., H. Miranda, O. Penn, T. Pupko, R. W. DeBry and D. Huchon (2009). "Rodent phylogeny revised: analysis of six nuclear genes from all major rodent clades." BMC Evol Biol **9**(1): 71.
- Bouxsein, M. L., S. K. Boyd, B. A. Christiansen, R. E. Guldberg, K. J. Jepsen and R. Müller (2010). "Guidelines for assessment of bone microstructure in rodents using micro-computed tomography." J Bone Min Res **25**(7): 1468-1486.
- Cook, M. J. (1965). The anatomy of the laboratory mouse, London (& New York): Academic Press.
- Corsortium, M. G. S., R. H. Waterston, K. Lindblad-Toh, E. Birney, J. Rogers, J. F. Abril, P. Agarwal, R. Agarwala, R. Ainscough, M. Alexandersson, P. An, S. E. Antonarakis, J. Attwood, R. Baertsch, J. Bailey, K. Barlow, S. Beck, E. Berry, B. Birren, T. Bloom, P. Bork, M. Botcherby, N. Bray, M. R. Brent, D. G. Brown, S. D. Brown, C. Bult, J. Burton, J. Butler, R. D. Campbell, P. Carninci, S. Cawley, F. Chiaromonte, A. T. Chinwalla, D. M. Church, M. Clamp, C. Clee, F. S. Collins, L. L. Cook, R. R. Copley, A. Coulson, O. Couronne, J. Cuff, V. Curwen, T. Cutts, M. Daly, R. David, J. Davies, K. D. Delehaunty, J. Deri, E. T. Dermitzakis, C. Dewey,

- N. J. Dickens, M. Diekhans, S. Dodge, I. Dubchak, D. M. Dunn, S. R. Eddy, L. Elnitski, R. D. Emes, P. Eswara, E. Eyraas, A. Felsenfeld, G. A. Fewell, P. Flicek, K. Foley, W. N. Frankel, L. A. Fulton, R. S. Fulton, T. S. Furey, D. Gage, R. A. Gibbs, G. Glusman, S. Gnerre, N. Goldman, L. Goodstadt, D. Grafham, T. A. Graves, E. D. Green, S. Gregory, R. Guigo, M. Guyer, R. C. Hardison, D. Haussler, Y. Hayashizaki, L. W. Hillier, A. Hinrichs, W. Hlavina, T. Holzer, F. Hsu, A. Hua, T. Hubbard, A. Hunt, I. Jackson, D. B. Jaffe, L. S. Johnson, M. Jones, T. A. Jones, A. Joy, M. Kamal, E. K. Karlsson, D. Karolchik, A. Kasprzyk, J. Kawai, E. Keibler, C. Kells, W. J. Kent, A. Kirby, D. L. Kolbe, I. Korf, R. S. Kucherlapati, E. J. Kulbokas, D. Kulp, T. Landers, J. P. Leger, S. Leonard, I. Letunic, R. Levine, J. Li, M. Li, C. Lloyd, S. Lucas, B. Ma, D. R. Maglott, E. R. Mardis, L. Matthews, E. Mauceli, J. H. Mayer, M. McCarthy, W. R. McCombie, S. McLaren, K. McLay, J. D. McPherson, J. Meldrim, B. Meredith, J. P. Mesirov, W. Miller, T. L. Miner, E. Mongin, K. T. Montgomery, M. Morgan, R. Mott, J. C. Mullikin, D. M. Muzny, W. E. Nash, J. O. Nelson, M. N. Nhan, R. Nicol, Z. Ning, C. Nusbaum, M. J. O'Connor, Y. Okazaki, K. Oliver, E. Overton-Larty, L. Pachter, G. Parra, K. H. Pepin, J. Peterson, P. Pevzner, R. Plumb, C. S. Pohl, A. Poliakov, T. C. Ponce, C. P. Ponting, S. Potter, M. Quail, A. Reymond, B. A. Roe, K. M. Roskin, E. M. Rubin, A. G. Rust, R. Santos, V. Sapojnikov, B. Schultz, J. Schultz, M. S. Schwartz, S. Schwartz, C. Scott, S. Seaman, S. Searle, T. Sharpe, A. Sheridan, R. Shownkeen, S. Sims, J. B. Singer, G. Slater, A. Smit, D. R. Smith, B. Spencer, A. Stabenau, N. Stange-Thomann, C. Sugnet, M. Suyama, G. Tesler, J. Thompson, D. Torrents, E. Trevaskis, J. Tromp, C. Ucla, A. Ureta-Vidal, J. P. Vinson, A. C. Von Niederhausern, C. M. Wade, M. Wall, R. J. Weber, R. B. Weiss, M. C. Wendl, A. P. West, K. Wetterstrand, R. Wheeler, S. Whelan, J. Wierzbowski, D. Willey, S. Williams, R. K. Wilson, E. Winter, K. C. Worley, D. Wyman, S. Yang, S. P. Yang, E. M. Zdobnov, M. C. Zody and E. S. Lander (2002). "Initial sequencing and comparative analysis of the mouse genome." Nature **420**(6915): 520-562.
- Dechant, J. E., G. M. Baxter, D. D. Frisbie, G. W. Trotter and C. W. McIlwraith (2005). "Effects of glucosamine hydrochloride and chondroitin sulphate, alone and in combination, on normal and interleukin-1 conditioned equine articular cartilage explant metabolism." Equine Vet J **37**(3): 227-231.
- Duce, S., L. Madrigal, K. Schmidt, C. Cunningham, G. Liu, S. Barker, G. Tennant, C. Tickle, S. Chudek and Z. Miedzybrodzka (2010). "Micro-magnetic resonance imaging and embryological analysis of wild-type and pma mutant mice with clubfoot." J Anat **216**(1): 108-120.
- Dyce, K. M., W. O. Sack and C. J. G. Wensing (2010). Textbook of veterinary anatomy. St. Louis, MO, Saunders/Elsevier.
- Gillis, G. B. and A. A. Biewener (2001). "Hindlimb muscle function in relation to speed and gait: in vivo patterns of strain and activation in a hip and knee extensor of the rat (*Rattus norvegicus*)." J Exp Biol **204**(15): 2717-2731.

- Glasson, S. S., R. Askew, B. Sheppard, B. Carito, T. Blanchet, M. Hak-Ling, C. R. Flannery, D. Peluso, K. Kanki and Z. Yang (2007). "Deletion of active ADAMTS5 prevents cartilage degradation in a murine model of osteoarthritis." Nature **446**(7131): 102.
- Grüneberg, H. and A. J. Lee (1973). "The anatomy and development of brachypodism in the mouse." J Embryol Exp Morphol **30**(1): 119-141.
- Nomenclature, V. G. A. (2012). Veterinary Gross Anatomical Nomenclature. General Assembly of the World Association of Veterinary Anatomists Editorial Committee, Hannover, Germany.
- Patton, J. and M. Kaufman (1995). "The timing of ossification of the limb bones, and growth rates of various long bones of the fore and hind limbs of the prenatal and early postnatal laboratory mouse." J Anat **186**(Pt 1): 175.
- Popesko, P., V. Rajtová and J. Horák (1992). A colour atlas of the anatomy of small laboratory animals. London, Wolfe Pub.
- Rose, S., E. A. Waters, C. R. Haney, C. T. J. Meade and H. Perlman (2013). "High-Resolution Magnetic Resonance Imaging of Ankle Joints in Murine Arthritis Discriminates Inflammation and Bone Destruction in a Quantifiable Manner." Arthritis Rheum **65**(9): 2279-2289.
- Rugh, R. (1968). The mouse: its reproduction and development. New York, Oxford England.
- Seemann, P., R. Schwappacher, K. W. Kjaer, D. Krakow, K. Lehmann, K. Dawson, S. Stricker, J. Pohl, F. Plöger and E. Staub (2005). "Activating and deactivating mutations in the receptor interaction site of GDF5 cause symphalangism or brachydactyly type A2." J Clin Invest **115**(9): 2373-2381.
- Settle, S. H., R. B. Rountree, A. Sinha, A. Thacker, K. Higgins and D. M. Kingsley (2003). "Multiple joint and skeletal patterning defects caused by single and double mutations in the mouse Gdf6 and Gdf5 genes." Dev Biol **254**: 116-130.
- Shubin, N., D. B. Wake and A. J. Crawford (1995). "Morphological Variation in the Limbs of *Taricha granulosa* (Caudata: Salamandridae): Evolutionary and Phylogenetic Implications." Evolution **49**(5): 874-884.
- Storm, E. E., T. V. Huynh, N. G. Copeland, N. A. Jenkins, D. M. Kingsley and S. J. Lee (1994). "Limb alterations in brachypodism mice due to mutations in a new member of the TGF beta-superfamily." Nature **368**(6472): 639-643.
- Tassabehji, M., Z. M. Fang, E. N. Hilton, J. McGaughran, Z. Zhao, C. E. de Bock, E. Howard, M. Malass, D. Donnai and A. Diwan (2008). "Mutations in GDF6 are associated with vertebral segmentation defects in Klippel-Feil syndrome." Hum Mutat **29**(8): 1017-1027.

- Wilson, L. A., C. Schradin, C. Mitgutsch, F. C. Galliari, A. Mess and M. R. Sánchez-Villagra (2010). "Skeletogenesis and sequence heterochrony in rodent evolution, with particular emphasis on the African striped mouse, *Rhabdomys pumilio* (Mammalia)." Org Divers Evol **10**(3): 243-258.
- Yakatan, G. J., W. J. Poynor, R. L. Talbert, B. F. Floyd, C. L. Slough, R. S. Ampulski and J. J. Benedict (1982). "Clodronate kinetics and bioavailability." Clin Pharmacol Ther **31**(402-410).

CHAPTER 5. CONCLUDING REMARKS

5.1 Overall Summary of Findings

The use of imaging in veterinary medicine has greatly advanced orthopedic research for both research and education purposes. This dissertation utilized one of these advanced imaging techniques, microCT, to analyze bone morphology in two animal models, answering several relevant questions in veterinary orthopedics: the effect of two FDA-approved bisphosphonate therapies (i.e. tiludronate and clodronate) on bone morphology and remodeling in horses, and the presence of tarsal variation in laboratory mice. In addition, this dissertation describes a novel, non-terminal bone biopsy method in the horse, providing the largest bone sample when compared to other methods previously described.

In Chapters 2 and 3, the aforementioned bone biopsy model was utilized to collect bone samples from the tuber coxae of young, clinically healthy horses. Bone samples were analyzed via microCT and histomorphometry to determine the effect of clodronate and tiludronate on bone structure and remodeling. In addition, the effect of clodronate on bone healing after a bone defect was analyzed. We determined that tiludronate and clodronate, administered at the recommended dose, do not have an effect on bone morphology or bone remodeling after 60 days in young horses. However, tiludronate and clodronate may have prevented minor bony changes, as seen in the control group, from occurring in the treated horses. Additionally, clodronate does not appear to impact bone healing 60 days following creation of a defect.

In Chapter 4, we characterized the bony tarsal anatomy in two common strains of laboratory mice (i.e., Black6 and BalbC), and compared this anatomy to selected

outgroups: the closely-related laboratory rat and the distantly related white-footed mouse. Utilizing microCT and histology, we confirmed that the central and tarsal bone III were fused in all laboratory mice evaluated. This fusion was not present in the rat or white-footed mouse. Histological sections showed the presence of hyaline cartilage surrounded by mature, trabecular bone. We conclude that although the bone is fused in these mice, a joint remnant remains.

5.2 Significance of Research

Assessment of bone health through bone biopsies in many species, including horses, is typically accomplished through obtaining a core biopsy from the sternbrae, ribs, third metacarpal bone, fourth tarsal bone and tuber coxae (Misheff et al., 1992, Steiger et al., 1999, Désévaux et al., 2000, Delguste et al., 2011), which has been shown to have poor trabecular bone for histological evaluation (Steiger et al., 1999). The biopsy method described in this dissertation produced biopsies almost 9 times larger than previously described biopsy volumes from other locations (Savage et al., 1991, Misheff et al., 1992, Steiger et al., 1999), with no associated morbidity or post-surgical lameness. Additionally, we showed that the biopsy model proposed in the current studies allows one to obtain sequential biopsies, permitting evaluation of bone across several time points.

Currently, tiludronate and clodronate are used extensively in the veterinary clinical setting to treat abnormal bone remodeling diseases (Denoix et al., 2003), including to young horses (Carpenter, 2012), which are known to undergo more rapid bone remodeling than skeletally-mature adults (Goyal et al., 1981). Despite the wide

use of clodronate in the clinical setting, and it's known systemic impact on the entire skeleton, there has been little to no research evaluating the effect of these drugs on normal bone remodeling in horses. Additionally, the effect of these drugs in young horses, who may be skeletally immature and undergoing increased bone remodeling and growth secondary to normal development, has not been evaluated. Our research shows that these drugs have minimal to no short-term effect on normal bone structure and remodeling in young horses. Additionally, we showed that in the presence of a bone defect, clodronate does not negatively affect normal bone remodeling after 60 days.

Rodent models are used for a variety of orthopedic research applications, including characterization of pathologic bony changes secondary to disease (Eulderink et al., 1998, Ford-Hutchinson et al., 2003, Goupil et al., 2016). Therefore, correct representations of normal bony anatomy are crucial in determining normal characteristics versus pathologic characteristics. Additionally, surgical procedures are guided by current knowledge of anatomy. Standard references for mouse anatomy show the mouse tarsus containing 8 individual bones (Cook, 1965), while a recent atlas of the mouse, utilizing microCT, demonstrated a fusion between two bones, and consisted of 7 individual bones (Bab et al., 2007). However, this atlas did not describe the fusion nor characterize it in relation to previous published anatomical descriptions of the tarsal region. Therefore, we were able to show that this fusion is present in two strains of wild-type laboratory mice. This fusion needs to be considered when studying diseases of the tarsus, or for surgical procedures involving the tarsus of mice.

5.3 Future Directions

The results presented in this dissertation show that tiludronate and clodronate do not affect bone structure and remodeling after 60 days. The next milestone of this project is to determine longer term effects of tiludronate and clodronate on bone, as well as increase sample size to determine if lesser effects exist. Additionally, due to their minimal effect shown in this study, the effect of tiludronate and clodronate on diseased bone in horses, specifically associated with navicular disease, needs to be evaluated as well, to determine the efficacy of these BPs.

We showed that fusion of the central and tarsal bone III is a normal characteristic in two strains of wild-type laboratory mice. Therefore, the next goal of this project is to evaluate additional individuals to increase sample size of the BalbC strain, as well as evaluate additional wild-type strains. Moreover, evaluating individuals from various mouse colony populations will help elucidate the extent of the fusion into all laboratory mice populations. Further evaluation of the anatomical extent of the fusion is also necessary, to determine if surrounding musculature and neurovasculature are affected. Finally, once affected mouse strains are known, determining genetic differences between mice with a fused bone versus mice without will facilitate researchers in determining the cause of the fusion, and possible interactions with future studies evaluating genetic manipulations or pathology.

5.4 References



Bab, I. A., C. Hajbi-Yonissi, Y. Gabet and R. Müller (2007). Micro-tomographic atlas of the mouse skeleton, Springer Science & Business Media.



- Carpenter, R. (2012). How to treat dorsal metacarpal disease with regional tiludronate and extracorporeal shock wave therapies in Thoroughbred racehorses. AAEP Annual Convention.
- Cook, M. J. (1965). The anatomy of the laboratory mouse, London (& New York): Academic Press.
- Delguste, C., M. Doucet, A. Gabriel, J. Guyonnet, O. M. Lepage and H. Amory (2011). "Assessment of a bone biopsy technique for measuring tiludronate in horses: a preliminary study." Can J Vet Res **75**(2): 128-133.
- Denoix, J. M., D. Thibaud and B. Riccio (2003). "Tiludronate as a new therapeutic agent in the treatment of navicular disease: a double-blind placebo-controlled clinical trial." Equine Vet J **34**(4): 407-413.
- Désévaux, C., S. Laverty and B. Doizé (2000). "Sternal bone biopsy in standing horses." Vet Surg **29**: 303-308.
- Eulderink, F., P. Ivanyi and S. Weinreich (1998). "Histopathology of murine ankylosing enthesopathy." Pathol Res Pract **194**(11): 797-803.
- Ford-Hutchinson, A. F., D. M. Cooper, B. Hallgrímsson and F. R. Jirik (2003). "Imaging skeletal pathology in mutant mice by microcomputed tomography." J Rheumatol **30**(12): 2659-2665.
- Goupil, B. A., M. A. McNulty, M. J. Martin, M. K. McCracken, R. C. Christofferson and C. N. Mores (2016). "Novel lesions of bones and joints associated with chikungunya virus infection in two mouse models of disease: new insights into disease pathogenesis." PLoS One **11**(5): e0155243.
- Goyal, H., F. MacCallum, M. Brown and J. Delack (1981). "Growth rates at the extremities of limb bones in young horses." Can Vet J **22**(2): 31.
- Misheff, M. M., S. M. Stover and R. R. Pool (1992). "Corticocancellous bone biopsy from the 12th rib of standing horses." Vet Surg **21**(2): 133-138.
- Savage, C. J., L. B. Jeffcott, F. Melsen and L. C. Ostblom (1991). "Bone biopsy in the horse. 1. Method using the wing of ilium." Zentralbl Veterinarmed A **38**(10): 776-783.
- Steiger, R. H., H. Geyer, A. Provencher, M. F. Perron-Lepage, B. von Salis and O. M. Lepage (1999). "Equine bone core biopsy: evaluation of collection sites using a new electric drilling machine." Equine Practice **21**: 14-21.

APPENDICES

Appendix A: First author, Colin F. Mitchell, provided permission for the second author to reuse material from article 'Assessment of Tuber Coxae Bone Biopsy in the Standing Horse'.

Colin Mitchell @
To: Heather Richbourg
RE: Use of 'Assessment of Tuber Coxae Bone Biopsy in the Standing Horse'

January 17, 2017 at 12:12 PM
Inbox - Exchange  

 Updated contact info found in this email: Colin F Mitchell (225) 578-9500 [update...](#) 

Heather,
You have my permission to reuse the published material in your thesis.
Colin

LSU

Dr Colin Mitchell, MS, Dipl ACVS
Associate Professor, Equine Surgery
Veterinary Clinical Sciences
Louisiana State University
School of Veterinary Medicine, Baton Rouge, LA 70803
office 225-578-9500 | fax 225-578-9605
cmitchel@lsu.edu | lsu.edu

From: Heather A Richbourg
Sent: Tuesday, January 17, 2017 10:34 AM
To: Colin F Mitchell
Subject: Use of 'Assessment of Tuber Coxae Bone Biopsy in the Standing Horse'

Dr. Mitchell,

I am writing to ask for your permission as first author to reuse material published in the article 'Assessment of Tuber Coxae Bone Biopsy in the Standing Horse,' published in the journal *Veterinary Surgery*. I will be reusing sections of the said article that I participating in and assisted in writing as the second author, (i.e., the introduction and materials and methods sections) in my dissertation, entitled 'Micro-Computed Tomography and Histological Evaluations of Bone in Equine and Muroid Models.'

Thank you for your collaboration and I look forward to hearing from you.

Heather A. Richbourg
PhD Candidate
Vice-President | The Graduate Student Organization at SVM
Dept. of Comparative Biomedical Sciences
Louisiana State University
Skip Bertman Drive, Baton Rouge, LA 70803
office 225-578-9745
hrichb1@lsu.edu | lsu.edu | [MicroCT Lab](#)

Appendix B: Veterinary Surgery is a member of John Wiley and Sons, which provides reuse or repurposing of articles with permission.

**JOHN WILEY AND SONS LICENSE
TERMS AND CONDITIONS**

Feb 01, 2017

This Agreement between Heather A Richbourg ("You") and John Wiley and Sons ("John Wiley and Sons") consists of your license details and the terms and conditions provided by John Wiley and Sons and Copyright Clearance Center.

License Number	4040230737800
License date	Feb 01, 2017
Licensed Content Publisher	John Wiley and Sons
Licensed Content Publication	Veterinary Surgery
Licensed Content Title	Assessment of tuber coxae bone biopsy in the standing horse
Licensed Content Author	Colin F. Mitchell, Heather A. Richbourg, Brad A. Goupil, Ashley N. Gillett, Margaret A. McNulty
Licensed Content Date	Jan 23, 2017
Licensed Content Pages	1
Type of use	Dissertation/Thesis
Requestor type	Author of this Wiley article
Format	Print and electronic
Portion	Full article
Will you be translating?	No
Title of your thesis / dissertation	Micro-Computed Tomography and Histological Evaluations of Bone in Equine and Murine Models
Expected completion date	Apr 2017
Expected size (number of pages)	200
Requestor Location	Heather A Richbourg LSU SVM Skip Bertman Drive BATON ROUGE, LA 70803 United States Attn: Heather A Richbourg
Publisher Tax ID	EU826007151
Billing Type	Invoice
Billing Address	Heather A Richbourg LSU SVM Skip Bertman Drive

Appendix C: Anatomical Record is a member of John Wiley and Sons, which provides reuse or repurposing of articles with permission.

**JOHN WILEY AND SONS LICENSE
TERMS AND CONDITIONS**

Jan 11, 2017

This Agreement between Heather A Richbourg ("You") and John Wiley and Sons ("John Wiley and Sons") consists of your license details and the terms and conditions provided by John Wiley and Sons and Copyright Clearance Center.

License Number	4026010970870
License date	Jan 11, 2017
Licensed Content Publisher	John Wiley and Sons
Licensed Content Publication	The Anatomical Record: Advances in Integrative Anatomy and Evolutionary Biology
Licensed Content Title	Anatomical Variation of the Tarsus in Common Inbred Mouse Strains
Licensed Content Author	Heather A. Richbourg,Matthew J. Martin,Emma R. Schachner,Margaret A. McNulty
Licensed Content Date	Oct 31, 2016
Licensed Content Pages	1
Type of use	Dissertation/Thesis
Requestor type	Author of this Wiley article
Format	Print and electronic
Portion	Full article
Will you be translating?	No
Title of your thesis / dissertation	Micro-Computed Tomography and Histological Evaluations of Bone in Equine and Muroid Models
Expected completion date	Apr 2017
Expected size (number of pages)	200
Requestor Location	Heather A Richbourg LSU SVM Skip Bertman Drive BATON ROUGE, LA 70803 United States Attn: Heather A Richbourg
Publisher Tax ID	EU826007151
Billing Type	Invoice
Billing Address	Heather A Richbourg LSU SVM Skip Bertman Drive

VITA

Heather Ashley Richbourg was born in March 1991 to Jeff Richbourg and Helen Caissie in Tallahassee, Florida. She attended Hayesville High School in Hayesville, NC. She competed in varsity Track and Field and Cross Country, earning three State Championship titles and two school records. She graduated 3rd in her high school class in May 2009. She then attended Young Harris College in Young Harris, Georgia, and majored in Biology and minored in Mathematics. While there, she competed in collegiate Cross Country and was a mathematics tutor. She earned her Bachelor of Science degree with Magna Cum Laude honors in May 2013. Heather then began her doctoral studies at the Louisiana State University School of Veterinary Medicine in 2013. Under the guidance of Dr. Margaret McNulty, Heather anticipates receiving her Doctor of Philosophy degree in May 2017 and will begin a postdoctoral position at the University of California at San Francisco in San Francisco, California.